Japan Geoscience Union Meeting 2015
(May 24th - 28th at Makuhari, Chiba, Japan)

SSS30-01 Room:A05 Time:May 25 09:00-09:15

Shear stress distributions of a subduction zone as inferred from elastic plate models

YOSHIDA, Mitsuru[1*]

[1]none

It is important to understand shear stress and fracture strength of a sesismogenic zone for the study of a seismogenesis mechanism. Shear stress characterisics of elastic oceanic and continental plates near a subduction zone are investigated using 2D finte element method in the case of plane strain. The present elastic plate model UMB-Plate (Figure) is composed of oceamic plate (Plate 1), continental plate (Plate 2), upper mantle (LMS), and two transitional layers, a plate boundary (PB) layer between Plate 1 and Plate 2 and an upper mantle boundary (UMB) layer between LMS and Plate 1. The two transitional layers correspond to low viscosity layers.

The Young's modulai (E) and Poisson's ratios (p) for Plate 1, Plate 2, and LMS are adopted from those used in the study of earthquake cycle simulation in Southwest Japan (Hori, et al., 2004). The Young's modulus is calculated from the rigidity (G) using the formula E=2(1+p)G (Tokawa, 1980). Young's modulus of mild steel of rubber-like-elasticity (Rikagakuziten, 1988) and Poisson's ratio of elastic rubber (Rika nenpyo, 2002) are used for those of PB and UMB. The size of the model is 625 and 325 mm in x- and y-directions, respectively, the thickness being 2 mm. The lengths enlarged to 200,000 times are ahown in the figure. A horizontal compressive force of 1.4 ton corresponding to a ridge push force of 4.7 MPa is applied to the left side of Plate 1. The right side of Plate 2 is fixed. The right side of Plate 1 is firstly assumed to be stress free. The dip angle of the subducting oceanic plate (Plate 1) is 10 deg. at shallow parts between sites C and I and 27 dig. at deeper parts between sites I and X. Site I corresponds to a convergent boundary.

The shear stresses calculated for UMB-Plate show that they are positive as a whole for Plate 2 above PB and are mostly negative for Plate 1. A positive shear stress zone exists in the inner part of Plate 1 at depths of 10-30 km beneath site C. The region showing a maximum shear stress of 1.095 MPa is located at edge of Plate 2 near site I. High shear stress zones are distributed at the thrust zone in Plate 2 above PB at depths less than 30 km. The region showing a minimum shear stress of -2.8x10E-06 MPa is located at a lower part of UMB near at a depth of 55 km. Mises stress defined by shear strain energy, which is one of the yield criterion (Kikuchi and Wada, 2004), is also highest at the left side of Plate 2 beneath site I, with a maximum stress of 19.25 MPa.

The elastic model UMB-Plate does not specify any particular region in Japanese island arc. However, the thickness 30 km and length 60 km of the oceanic plate is rather close to the vertical section of the crust and upper mantle in the Tokai district, Southwest Japan. If the slab is short the earthquake mechanism in the slab is likely to show a normal fault in the negative shear stress field and the thrust zone is characterized by a low-angle reverse fault in the positive shear stress field (Seno. 2001). The shear stress distributions calculated seem to be in harmony with the stress field mentioned above.

The effects of negative buoyancy which corresponds to a slab pull force were examined. If the downward pull force is applied to the right side of Plate 1, the area showing a positive shear stress increases inside the subducting Plate 1, while the area showing a negative shear stress increases inside Plate 2.

Figure. Configulation of elastic plate model UMB-Plate and elastic constants of media.

Keywords: Shear stress, Subduction zone, Elastic plate model, 2D FEM

Keywords: shear stress, subducion zone, elastic plate model, 2D FEM

SSS30-01 Room:A05 Time:May 25 09:00-09:15

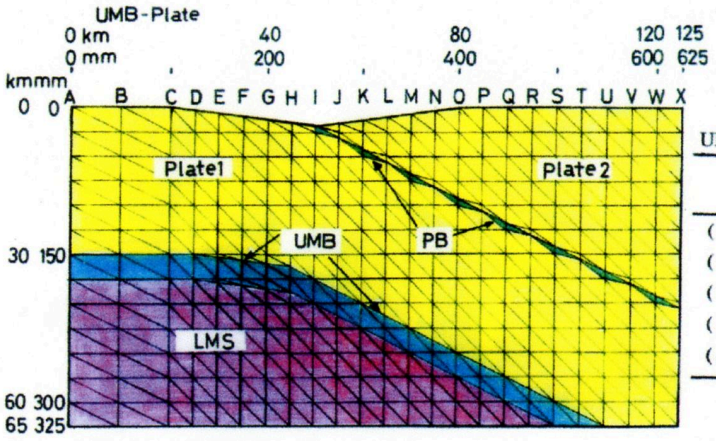

UMB-Plate

No.	Young's Modulus [MPa]	Poisson's ratio
(1) Plate 1	$1.65 * 10^5$	0.25
(2) Plate 2	$1.65 * 10^5$	0.25
(3) PB	1.65	0.46
(4) UMB	1.65	0.46
(5) LMS	$1.708 * 10^5$	0.298

Japan Geoscience Union Meeting 2015
(May 24th - 28th at Makuhari, Chiba, Japan)

SSS30-02 Room:A05 Time:May 25 09:15-09:30

Two-dimensional fully dynamic spectral-element simulations of long-term in-plane shear fault slip

SHIMIZU, Hiroyuki[1] ; KANEKO, Yoshihiro[2] ; HIRAHARA, Kazuro[1*]

[1]Graduate School of Science, Kyoto University, [2]GNS Science

Earthquake cycle simulations have been performed to successfully reproduce historical earthquake occurrences (eg. Tse and Rice 1986; Stuart, 1988). Most of them are based on a quasi-dynamic scheme, where inertial effects are approximated by the radiation damping term proposed by Rice (1993). This is because a “fully-dynamic” scheme that accounts for all the inertial effects requires quite large CPU and memory cost. Lapusta et al. (2000, 2009) developed a methodology capable of simulating seismic and aseismic slip and gradual process of earthquake nucleation over the entire earthquake cycle. Their fully-dynamic simulations have produced earthquake cycles considerably different from quasi-dynamic ones (Thomas et al., 2014). Those simulations have, however, never been performed for interplate earthquakes at subduction zones, because their models based on a spectral boundary integral method are currently limited to relatively simple fault geometry.

Many studies showed that, for rupture on a dipping fault such as interplate earthquakes at subduction zones, normal stress is altered during faulting due to the interaction with the Earth’s free surface. This change in normal stress not only affects the earthquake rupture process, but also causes the residual stress variation that might affect the long-term histories of earthquake cycles (Duan and Oglesby, 2005). Therefore it is important to account for both the dipping fault geometry and the dynamic effects.

Recently, Kaneko et al. (2011) have performed the fully dynamic spectral-element method (SEM) simulations of the long-term anti-plane fault slip. They combined quasi-static and fully-dynamic SEM schemes for simulating entire earthquake cycles. Aiming at simulating interplate earthquake cycles at subduction zones, we extend their study to simulations for in-plane shear faults and implement our numerical scheme in a dynamic rupture SEM code (Ampuero, 2002). Unlike the anti-plane cases, an in-plane shear fault requires modifications of the fault-perpendicular displacements, which were neglected in Kaneko et al. (2011). While this is implicitly calculated in BIEM (Boundary Integral Equation Method) simulations, we have to explicitly update such values in the domain method like SEM.

We perform fully-dynamic earthquake cycle simulations of long-term slip on a simple planar fault embedded in an elastic medium as described in Kaneko et al. (2011; Fig.2) except that we consider an in-plane fault and use quasi-dynamic updating scheme during the interseismic periods. The central portion of the fault is governed by the rate-and-state friction and both sides of the fault are steady-sliding velocity boundaries. Our numerical code is verified by the convergence of the results with several different discretization sizes, and by approximately the same recurrence times for the cases of anti-plane and in-plane faults, where the same nucleation sizes are obtained by adjusting frictional parameters. The code also works well for a vertical fault in an elastic half space. We discuss the differences between the dynamic and quasi-dynamic simulations.

We also discuss applications of our updated SEM scheme to the dipping fault. For dipping fault rupture such as the 2011 Tohoku earthquake in a homogeneous elastic half-space, we successfully simulate scenarios of single dynamic rupture propagation. However, we have some problems in simulating quasi-static interseismic simulations at present for this case.

Keywords: computational seismology, earthquake cycle, rate and state friction law, spectral element method, fully dynamic, interplate earthquake

Japan Geoscience Union Meeting 2015
(May 24th - 28th at Makuhari, Chiba, Japan)

SSS30-03 Room:A05 Time:May 25 09:30-09:45

Forecast experiments using friction law on occurrence times of the Kamaishi repeating earthquakes

YOSHIDA, Shingo[1*] ; KATO, Naoyuki[1] ; FUKUDA, Jun'ichi[1]

[1]ERI, Univ. Tokyo

Uchida et al. (2014) reported that a repeating earthquake sequence on the plate boundary off the shore of Kamaishi showed a regular recurrence interval before the 2011 Tohoku-oki earthquake (M9). After the Tohoku-oki earthquake, the repeaters showed increases in magnitude and shorter recurrence intervals. A M6 class event occurred just after the M9 event. Uchida et al. (2014) proposed a conceptual model in which conditionally stable regions and unstable regions are distributed. Using this model, Yoshida, Kato, and Fukuda (2015) conducted numerical simulations of the Kamaishi repeaters assuming the afterslip obtained by Fukuda et al (2013). In this simulation, a M6 class event was reproduced, and the calculated occurrence times of the following repeaters resembled the observation to some degree.

In this study, we perform trial experiments on occurrence time forecast of the Kamaishi repeaters. 11 events occurred after the M9 events. Assuming various parameters, we calculate the occurrence times of the 10 events before the latest event. We select proper models by evaluating these models, and calculate the occurrence time of the 11th event using the selected models. Average of the calculated times would provide an estimate. We discuss how we should evaluate the models, and incorporate simulations into prediction schemes.

Keywords: Kamaishi repeaters, occurrence time, prediction experiment, numerical simulation, rate and state dependent friction law, afterslip

Japan Geoscience Union Meeting 2015
(May 24th - 28th at Makuhari, Chiba, Japan)

SSS30-04 Room:A05 Time:May 25 09:45-10:00

Adequate Emplacement of the Data Assimilation Window and Sensitivity Analysis

HIYOSHI, Yoshihisa[1*] ; SUGIURA, Nozomi[1] ; HORI, Takane[1]

[1]JAMSTEC

Comprehension of fault behavior in earthquake sequence inevitably requires to elucidate frictional properties on slip interfaces. One of the good candidates to grasp the properties is data assimilation.

Recently Kano et al. (2013) developed a methodology for applying an adjoint-based data assimilation method to constrain some of the frictional properties on a simplified fault model with synthetic afterslip observation data. They found that all the frictional parameters were optimized when both acceleration and deceleration phases of the observed slip-rate data were assimilated. Importance of their finding is that an adequate emplacement of the assimilation time window plays one of the key roles to optimize the frictional parameters.

In this research, we attempt to find where the assimilation time window should be placed on to constrain all the frictional parameters. It could be acceptable that the assimilation time window should cover portions of the slip rate time series having the highest sensitivity to perturbations of the frictional properties. To ensure the above notion, we make theoretical and numerical approaches.

First, we set a simplified fault model with a rate- and state-dependent law and an aging law, sketching characteristics of the long-term slow slip events (SSEs) recurring on the plate interface beneath the Bungo Channel in southwest Japan.

For searching the portions of the highest sensitivity, we take a first variation of the governing equations of the SSE model. This algebraic manipulation shows that the highest sensitivity appears in the acceleration phase of the slip rate time series.

We then make a series of synthetic data assimilation experiments to examine whether or not the highest sensitivity portion offer an adequate assimilation window. The experiments employ an adjoint data assimilation method to constrain frictional parameters of the Bungo SSE model with synthetic slip rate observation data.

In our presentation, we will demonstrate the results of the experiments that the acceleration part of the slip rate is expected to be necessary to retrieve all the frictional parameters on the slip interfaces.

Combining the results of the mathematical formulation and the synthetic data assimilation experiments, we may confirm that an adequate assimilation time window spans the portions having the highest sensitivity to perturbations of the frictional parameters. Also, the distribution of the sensitivities in the slip rate time series could be obtained as a priori knowledge through the algebraic manipulation of the governing equations.

Keywords: data assimilation, sensitivity analysis, adjoint method

Japan Geoscience Union Meeting 2015
(May 24th - 28th at Makuhari, Chiba, Japan)

SSS30-05 Room:A05 Time:May 25 10:00-10:15

Power spectral density of slip distribution and slip rate function

HIRANO, Shiro[1*] ; YAGI, Yuji[2]

[1]University of Tsukuba, [2]University of Tsukuba

In view of energetics, earthquake faulting is a physical process that part of cumulated strain (i.e., potential) energy is converted into radiated (i.e., kinetic) energy. We have revealed that the potential energy and kinetic energy can be represented by quite similar spectral integrals although the former is with respect to spatial wavenumber and the latter is with respect to frequency[1]. In other words, power spectral densities (PSD) of the potential energy, which is correlated to slip distribution[2], and kinetic energy, which is correlated to slip rate function, are related to each other. This seems to be reasonable qualitatively because shorter wavelength components of the slip distribution should generate higher frequency contents of the seismic wave. To investigate this relationship quantitatively, we model spatio-temporal distribution of slip rate function on the fault and show that PSD of slip distribution and PSD of slip rate function should have the similar form. In our model, the distribution of slip rate function is represented as spatial distribution of peak slip velocity multiplied by a characteristic slip rate function that arises when the rupture front arrives at each point; this is an extension of the Haskell model. We find that the PSDs are proportional to a PSD of distribution of the peak slip velocity even if the distribution is quite heterogeneous and rupture velocity has perturbation in space. This suggests that the PSD of the slip distribution, which is hardly analyzed due to poor resolution of slip inversion analyses, can be roughly estimated by using the PSD of slip rate function of an ideal point source. Additionally, our model of the characterized slip rate function is consistent with a result of dynamic simulation of spontaneous rupture propagation along a rough fault[3]. Hence we suggest a simple method to estimate not only heterogeneity of slip distribution but also roughness of faults.

References

[1] Hirano, S., & Yagi, Y., 2014, Dependence of Seismic Energy on Higher Wavenumber Components, *AGU Fall Meeting*, S53B-4505.

[2] Mai, P.M., & Beroza, G.C., 2002, A Spatial Random Field Model to Characterize Complexity in Earthquake Slip, *J. Geophys. Res.*, **107**(B11) 2308.

[3] Trugman, D.T., & Dunham, E.M., 2014, A 2D Pseudodynamic Rupture Model Generator for Earthquakes on Geometrically Complex Faults, *Bull. Seism. Soc. Am.*, **104**(1) 95-112

Keywords: Slip inversion, Power spectral density, Earthquake energy budget, Heterogeneous fault

Japan Geoscience Union Meeting 2015
(May 24th - 28th at Makuhari, Chiba, Japan)

SSS30-06 Room:A05 Time:May 25 10:15-10:30

Fractal fault zone geometry and scale-dependent static stress drop

OTSUKI, Kenshiro[1*]

[1]Department of Geology, Graduate School of Science, Tohoku Univ.

I have shown that fault zone geometries, composed of fault segments and jog, are hierarchically selfsimilar (Fig.1a). This inhomogeneous structure breaks down the wellknown relations among fault length, averaged seismic slip and seismic moment. The distribution of seismic slip also is pinned hierarchically by jogs, showing a spectral distribution (Fig.1b). Based on the high quality data of fault traces and slip distributions from 21 surface earthquake strike-slip faults, here I show that average static stress drop $\triangle\sigma$ decreases as L_0.

Key Point 1
If $D_{av}$of a fault (L, D_{max}) is $\pi D_{max}/4$, $\triangle\sigma = C\pi D_{max}/4L$.
For a fault composed of linked n faults with (L/n, D_{max}) also $D_{av} = \pi D_{max}/4$, while $\triangle\sigma = nC\pi D_{max}/4L$.
[Symbol fault length:L, maximum slip:D_{max} and averaged slip:D_{av}, static stress drop:$\triangle\sigma$, proportional constant:C]

Key Point 2
Slip distributions D_x on fault segments are approximated by two simple cases below.
Cases of homogeneous frictional resistance $D_x = 2(1 - \nu)/G \times ({\sigma_{yx}}^r - {\sigma_{yx}}^c) \times (a^2 - x^2)^{0.5}$.
Cases of frictional resistance with a linear gradient $D_x = (1 - \nu)/G \times (2{\sigma_{yx}}^r - {\sigma_{yx}}^c(x/a)) \times (a^2 - x^2)^{0.5}$.
[Symbol half length of fault segments:a, Poisson's ratio:ν, remote stress:${\sigma_{xy}}^r$, frictional resistance:${\sigma_{xy}}^c$]

Key Point 3
When $L_s(i,j) < W_s$, $\triangle\sigma_{av}(i,j) = (7\pi G/8)(D_{av}(i,j)/L_s(i,j)$.
When $Ls(i,j) > W_s$, $\triangle\sigma_{av}(i,j) = (2G/\pi)(D_{av}(i,j)/W_s$.
The static stress drops averaged over the whole fault length L_0 is $\triangle\sigma = (\sum\triangle\sigma_{av}(i,j)L_s(i,j)/L_0$.
[Symbol for j-th segment of hierarchical rank i, segment length:$L_s(i,j)$, averaged slip:$D_{av}(i,j)$, static stress drop:$\triangle\sigma_{av}(i,j)$, thickness of seismogenic crustal layer:W_s, rigidity:G]

Analytical Results
17 among 21 data are approximated to the equation below (Fig.1c).
$\triangle\sigma = 79.0\ {L_0}^{-0.519}$ (units km and MPa)

Keywords: static stress drop, scale dependence, fault zone geometry, hierarchically selfsimilar

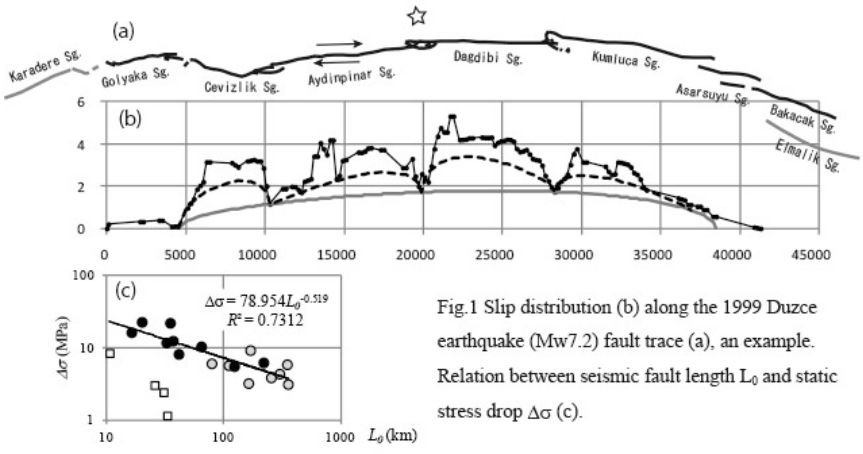

Fig.1 Slip distribution (b) along the 1999 Duzce earthquake (Mw7.2) fault trace (a), an example. Relation between seismic fault length L_0 and static stress drop $\Delta\sigma$ (c).

Japan Geoscience Union Meeting 2015
(May 24th - 28th at Makuhari, Chiba, Japan)

SSS30-07 Room:A05 Time:May 25 10:30-10:45

An arithmetic approach for modeling of seismic activity

FUJIWARA, Hiroyuki[1*]

[1]NIED

The ”arithmetic seismic activity model” is proposed by Fujiwara (2014) and the seismic activity is modeled by using the prime numbers to express the seismic activity that follows the G-R law as mathematical model. Although the ”arithmetic seismic activity model” is one that has been inferred from the phenomenological similarities between seismic activities and the prime number distributions, there may be some mathematical and physical meanings behind the model. Focusing on the relationship called trace formula, a study have been conducted.

We consider a correspondence between earthquakes and prime numbers. We parameterize occurrence time of earthquakes as the prime numbers and magnitude of earthquakes as the interval of prime numbers. Then we obtain a relationship similar to G-R law. We call the model obtained by this correspondence as ”arithmetic seismic activity model”. In the ”arithmetic seismic activity model”, earthquake is equivalent to prime number. Earthquake prediction is equivalent to prediction of emergence of prime numbers.

Trace formula is an equation obtained by calculating the trace of certain operator in two ways. A common feature in the trace formula, the sum on the prime elements in the geometric side is equal to the sum on the eigenvalues in the spectrum side. By generalizing these characteristics of the trace formula, it is possible to regard the explicit formula on prime numbers obtained by Riemann as one of the trace formula. Point processes in which points are irregularly occurred are difficult to handle in mathematical modeling. By using the trace formula, however, it is possible to express a point process as a sum of relatively simple continuous functions. Thus, by using the trace formula, an irregular point process is expected to be modeled as an eigenvalue problem of certain dynamical system.

An earthquake is understood as a phenomenon that corresponds to a change in the energy level of the field. Using certain quantum system, we consider to model a field of earthquake occurrence. Considering a Hamiltonian of the field of earthquake occurrence, we set earthquake occurrence as an eigenvalue problem for the Hamiltonian. If we can show that the eigenvalue problem is associated with the zeta function, we can expect to explain the similarity between the distribution of the prime and seismic activity. At present, any dynamical systems can explain seismic field based on this concept are not known. On the other hand, researches on the distribution of prime numbers are progressing to try to understand the distribution of zeros of the Riemann zeta function, which is equivalent to the distribution of prime number, as an eigenvalue problem of a quantum dynamical system.

Connes derived a trace formula of Selberg type by considering the operation of an idele class group on a square integrable function space that is defined on a space of adele class and showed that to prove the trace formula and to prove the Riemann conjecture are equivalent. Volovich proposed the p-adic quantum mechanics and considered an extension of quantum mechanics onto an adele space. As a part of their research, harmonic oscillators on an adele space are introduced and the Mellin transforms of them are shown to be expressed using the Riemann zeta function. Thus, eigenvalue problems of dynamical systems that are configured on an adele space are found to be associated naturally with the Riemann zeta function.

In this study, referring to the idea of extension of the quantum mechanics onto an adele space, we try to formulate the quantization (non-commutativization) of the continuum mechanics that gives the physical basis of seismology. On the basis of these basic studies, an attempt is made to regard earthquake oocuurence as eigenvalue problems of dynamical systems on an adele space.

Keywords: number theory, prime number, earthquake, trace formula, adele

Japan Geoscience Union Meeting 2015
(May 24th - 28th at Makuhari, Chiba, Japan)

SSS30-08 Room:A05 Time:May 25 11:00-11:15

Systematic Understanding of Dynamic Earthquake Slip Process in the System without Fluid Flow

SUZUKI, Takehito[1*] ; YAMASHITA, Teruo[2]

[1]Coll. Sci. & Eng., AGU, [2]ERI, Univ. Tokyo

We have explained many aspects of dynamic earthquake slip process by constructing the framework associated with the interaction among heat, fluid pressure and inelastic pore creation. We found three nondimensional parameters, Su, Su' and Ta, in the framework. In particular, Su describes the relative dominance of the effect of inelastic pore creation on the fluid pressure change over that of shear heating. In our previous studies, we analyzed the parameter range $Su>1-v_0^*$, where v_0^* is the initial value of the normalized slip velocity v^*. For this parameter range, we found the acceleration case and the spontaneous slip cessation case for the slip process. The acceleration case shows the transition from deceleration to acceleration with high-speed final slip, while the spontaneous slip cessation case shows the slip arrest with final zero stress drop. The former case corresponds to gradual acceleration phase (GAP) or a dynamic event preceding the main shock, while the latter indicates pulse-like slip for 2-D fault models. They are quantitatively distinguished by the value of the function G; if $G>0$, the acceleration case is observed, while if $G<0$, the spontaneous slip cessation case appears. We assume the parameter range $Su<1-v_0^*$ in the present study.

First, we found that the steady state value of the normalized slip velocity is zero or unity over a whole range of Su. In addition, deceleration at the initial stage of the slip is required to attain the steady state value zero. In the case $Su<1-v_0^*$, we found analytically that temporal differentiation of slip velocity is always positive, which leads to the conclusion that only acceleration occurs (the steady state value unity is realized) during the slip.

In this case, thermal pressurization is predominant over the pore creation, so that high-speed slip and complete stress drop are observed. Moreover, temperature increase is kept below the fault rock melting point. We found that these natures describe slip for the ordinary earthquakes with GAP and the high-speed slip and without the fault rock melting, which is the same behavior as those of $Su>1-v_0^*$ and $G>0$. It is also important here that, since the final porosity is less than the upper value, we can reproduce (i) non-negligible porosity generation, and (ii) temperature under the fault rock melting point, both of which have been seismologically fundamental requirements, as done in the case $Su>1-v_0^*$. The behavior in the system without the fluid flow is understood in a unified way for all values of Su.

Keywords: theory, heat, fluid pressure, pore creation, nonlinear, interaction

Japan Geoscience Union Meeting 2015
(May 24th - 28th at Makuhari, Chiba, Japan)

SSS30-09 Room:A05 Time:May 25 11:15-11:30

Generation of low-frequency tremor by fluid flow

SAKURABA, Ataru[1*]

[1]School of Science, University of Tokyo

We discuss the possibility that flow-induced instability along underground conduit or plane layer causes low-frequency tremor. One example is generation of volcanic tremor, which occurs before or during eruption and lasts more than a few minutes with oscillation period of 0.2-2 seconds (e.g., see Konstantinou and Schlindwein, *J. Volcanol. Geotherm. Res*., 2002). Sakuraba and Yamauchi (*Earth Planets Space*, 2014) showed that a relatively slow magma flow speed of O(1) m/s through a plate-like dike of thickness of around 0.5 m can cause linear instability in flow perturbation and surrounding elastic wave field. The critical magma flow speed decreases in inverse proportion to the Rayleigh-wave wavelength propagating along the dike with flexural deformation. They concluded that natural dike lengths put constraint on the oscillation period, but a subsequent study suggests that a finite dike width may determine the longest wavelength that allows instability. A laboratory experiment is also ongoing to verify the above theoretical prediction that a viscous fluid flow through a plate-like conduit can create self-oscillations. Another example may be found in generation of non-volcanic deep tremor that occurs at subducting plate (Obara, *Science*, 2002). This is still a speculation motivated from a study by Kumaran, Fredrickson and Pincus (*J. Phys. II France*, 1994) who considered Couette flow between two parallel plates, one of which is rigid and the other is moving, but the medium between the plates is two-layered: a fluid layer is placed on a layer of soft (viscoelastic) material. They theoretically showed that flow-induced vibration can occur with a very small shear rate. In an idealized situation in which the solid layer extends infinitely, the critical speed of the moving plate decreases in inverse proportion to the characteristic length scale of the associated wave that propagates at a half the plate speed. Though we have not examined whether this model explain time scales of observations with reasonable physical and material properties, similarity between the above mentioned examples suggests that flow-induced instability may explain some of the tremor events.

Keywords: flow-induced vibration, volcanic tremor, non-volcanic deep tremor

Japan Geoscience Union Meeting 2015
(May 24th - 28th at Makuhari, Chiba, Japan)

SSS30-10 Room:A05 Time:May 25 11:30-11:45

High-resolution tremor locations reveal behaviors of secondary slow slip fronts in the context of the main front

PENG, Yajun[1*] ; RUBIN, Allan[1]

[1]Department of Geosciences, Princeton Univeristy

Non-volcanic tremor is generally interpreted as the seismic manifestation of slow slip, and tremor locations have been used extensively to infer detailed behaviors of slow slip fronts due to higher spatial and temporal resolution over geodetic observations. Taking advantage of S-wave coherence among stations separated by roughly 10 km, we obtain high precision tremor locations in Cascadia using cross-station cross correlations, with either 3-station detectors (southern Vancouver), or 3-array detectors (Olympic Peninsula). We observe that near the main front, tremor migrations usually propagate along the main front, regardless of its orientation, and their recurrence intervals are too short to be tidally driven. Rapid tremor reversals (RTRs) originate from the main front, and sometimes start as migrations propagating along the main front. Although the occurrence of most of the RTRs appears to be correlated with high tidal shear stresses, we observe a few exceptions, which may suggest that the stress increase far behind the main front induced by secondary fronts at the main front is sometimes enough to initiate a RTR. Beneath Olympic peninsula, the spatial densities of tremor during the ETS and the inter-ETS events seem to be complementary, and RTRs do not often extend into regions that are de-stressed by the inter-ETS event.

Preliminary results of tremor locations beneath Guerrero, Mexico indicate that our method also performs well in this region. It seems that a tremor asperity about 50 km across ruptured quasi-periodically with a recurrence interval of ˜3 months until the 2006 slow slip event drastically decreased it.

Keywords: Episodic tremor and slip, Cascadia subduction zone, Mexican subduction zone, Cross-station method

Japan Geoscience Union Meeting 2015
(May 24th - 28th at Makuhari, Chiba, Japan)

SSS30-11 Room:A05 Time:May 25 11:45-12:00

Source parameters of foreshocks and aftershocks of 2014 Northern Nagano earthquake

IMANISHI, Kazutoshi[1*] ; UCHIDE, Takahiko[1]

[1]Geological Survey of Japan, AIST

The 2014 M6.7 Northern Nagano earthquake occurred on 22 November, 2014, which broke a part of Kamishiro fault. In order to reveal the generation mechanism of the mainshock, we determined hypocenters and source parameters of foreshock sequence from four days before the mainshock, as well as aftershocks.

We assumed two different one-dimensional crustal velocity structures to account for heterogeneous velocity structure in the studied area. Hypocenters are shifted by the relocation to the east at about 2 km and shallower at most 5 km, compared with the JMA catalogue. Although the aftershock distribution basically defines an eastward dipping plane, vertical and westward dipping planes are also identified at the middle to the northern part of the source region. The foreshocks located at about 3 km depth and distributed on NNW dipping plane, which is clearly distinct from the aftershock distribution. It is noted that the foreshock sequence started at the deeper part, then migrated to the shallower part and finally approached to the mainshock nucleation point.

We then determined focal mechanisms from P-wave polarity data as well as body wave amplitude, which enabled us to obtain well-determined solutions down to M0.5. Most of aftershocks exhibit a large strike-slip component, while aftershocks occurring at the southern part of the source region show reverse faulting type of mechanisms. This feature is consistent with the aftershock distribution. As for the foreshock sequence, we obtained a number of events with a large strike-slip component having a nodal plane dipping to the NNW, which is also consistent with the foreshock distribution. Interestingly, we found that the foreshock focal mechanisms slightly change with time and finally resemble to the P-wave first-motion mechanism of the mainshock. We detected more than 400 new events based on visual inspection of running spectra and S-P time at the station closest to the foreshock sequence (Hi-net Hakuba station). Hypocenter and focal mechanism determination of these events will further contribute to elucidate the relation between the foreshock sequence and the mainshock occurrence.

We will also present the stress drop estimations and discuss the spatial distribution of stress drops as well as the difference in source properties between the foreshocks and aftershocks.

Acknowledgements: Seismograph stations used in this study include permanent stations operated by NIED (Hi-net), JMA, ERI, and DPRI.

Keywords: Northern Nagano earthquake, source parameter, foreshock, aftershock

Japan Geoscience Union Meeting 2015
(May 24th - 28th at Makuhari, Chiba, Japan)

SSS30-12 Room:A05 Time:May 25 12:00-12:15

Source process of the 2014 Northern Nagano earthquake

KOBAYASHI, Hiroaki[1*] ; KOKETSU, Kazuki[1] ; MIYAKE, Hiroe[1]

[1]Earthquake Research Institute, University of Tokyo

An earthquake with JMA magnitude 6.7 occurred on 22 November, 2014, in the northern Nagano prefecture, Japan. This earthquake caused 46 casualties and damaged over 1500 housings. GCMT, F-net and JMA-CMT solution are coincide with each other and shows that a focal mechanism of this earthquake is reverse fault with some strike-slip components and about 20% non-DC component. Immediately after the earthquake, various institutions conducted field surveys and reported surface faults. Because the surface fault traces mostly matched with a known active fault named the Kamishiro fault, this fault is thought to be ruptured during the earthquake. The Kamishiro fault is located at the northern part of the Itoigawa-Shizuoka Tectonic Line which is one of the largest fault zones in Japan. It is important to investigate the source process of the earthquake. We performed a joint inversion of strong-motion and geodetic data to understand the source process of the earthquake.

In the northern Nagano region, there are dense strong-motion observation networks of K-NET, KiK-net, SK-net, and ERI. We used 45 components at 15 stations for the source inversion. All the waveforms were integrated to velocity, band-pass filtered between 0.02 - 0.4 Hz, and resampled with 0.25 s. For geodetic data, we chose 9 stations from GEONET. We used the daily coordinates of the F3 solution (Nakagawa et al., 2009) of GSI. To calculate static displacement by the earthquake, we set GEONET Shirotori as a reference point and then compared the mean value of 2-6 days before and after the earthquake. We used horizontal components and three components for GEONET Hakuba where significant vertical displacement was observed.

We used inversion methods of Yoshida et al. (1996) and Hikima and Koketsu (2005). Strong-motion Green's functions were calculated by the method of Kohketsu (1985) with one-dimensional velocity structure model based on the Japan Integrated Velocity Structure Model [JIVSM] (Koketsu et al., 2008, 2012) for each station. Geodetic Green's functions were calculated by the method of Zhu and Rivera (2002). In this calculation, a one dimensional velocity structure model beneath the GEONET Hakuba was extracted from the JIVSM and used for all the stations. We divided the faults into 13 x 7 subfaults and set strike and dip angles considering the surface faults and aftershock distributions. Each subfault has a size of 2 km x 2 km with a point source at the center with rake angle of 45±45 to represent from reverse to left-lateral strike-slip faulting.

We obtained largest slip located at the north-eastern deeper part of the hypocenter. The shallower part has also some slips with maximum at near GEONET Hakuba. This slip area coincides with the observed largest surface displacement point. However, the focal mechanism calculated by summing up obtained slip vectors cannot explain the non-DC component, suggesting further investigation needed.

Keywords: 2014 Northern Nagano earthquake, source process, source inversion

Japan Geoscience Union Meeting 2015
(May 24th - 28th at Makuhari, Chiba, Japan)

SSS30-13 Room:A05 Time:May 25 12:15-12:30

Dynamic rupture model of the 2014 northern Nagano, central Japan, earthquake

KASE, Yuko[1*]

[1]Geological Survey of Japan, AIST

The 2014 northern Nagano, central Japan, earthquake (M_{JMA}6.7) occurred in November 22, 2014. The surface ruptures intermittently observed along the Kamishiro fault (Katsube, this meeting), but the southern part of the fault remains to be ruptured. We construct a dynamic rupture model of the earthquake to understand the mechanism of the earthquake and the present condition of the fault.

Fault length and lower depth of the fault is 22 km and 15 km, respectively, based on the aftershock distribution (JMA, 2014; NIED, 2014) and InSAR image (GSI, 2015). Fault strike is N10E, based on the aftershock distribution and the strike of the Kamishiro fault (MEXT et al., 2004). Dip angle of the deeper region than 2 km is 60 degrees, based on the CMT solutions (JMA, 2014; NIED, 2014) and aftershock distribution, and dip angle of the shallower region than 2 km is 45 degrees, based on the analysis of the InSAR data (Yarai, 2015). The southern part of the fault reaches the earth's surface, while upper depth of the northern part is 2 km. Principal stresses are proportional to depth. Azimuth of the maximum principal stress is N65W (MEXT et al., 2004). The minimum principal stress is vertical, and equal to overburden load. We assume hydrostatic condition. The medium has 2-layered structure with 2 km-depth boundary, based on the subsurface structure model around the fault (NEID, 2003). The upper layer has zero stress drop, since it corresponds to sediment layer. We calculate dynamic rupture processes by the finite-difference method (Kase, 2010), assuming the slip-weakening friction law, and search average stress drop that is consistent with the observed seismic moment.

In case that the average stress drop is 3.3 MPa, the seismic moment is 6.21 x 10^{18} Nm (Mw6.5), which is almost agree with the CMT solutions. Rupture first smoothly propagates, because our dynamic rupture model is laterally homogeneous. After the rupture reaches 2 km-depth, the rupture suddenly decelerates because of zero stress drop. The maximum slip on the fault is about 2 m, and the maximum surface slip is about 1.1 m, which is agree with the observed one (Hirouchi et al., 2014).

Keywords: dynamic rupture, 2014 northern Nagano earthquake, Kamishiro fault, numerical simulation

Japan Geoscience Union Meeting 2015
(May 24th - 28th at Makuhari, Chiba, Japan)

SSS30-14 Room:A05 Time:May 25 14:15-14:30

Fault strength in Marmara region inferred from the geometry of the principle stress axes and fault orientations

PINAR, Ali[1*] ; COSKUN, Zeynep[1] ; MERT, Aydin[1] ; KALAFAT, Dogan[1]

[1]Bogazici University Kandilli Observatory and Earthquake Research Institute

The general consensus based on historical earthquake data suggests that the last major moment release on the Prince's islands fault was in 1766 which in turn points out an increased seismic risk for Istanbul Metropolitan area considering the fact that most of the 20 mm/yr GPS derived slip rate for the region is accommodated mostly by that fault segment.

The orientation of the Prince's islands fault segment overlaps with the NW-SE direction of the maximum principle stress axis derived from the focal mechanism solutions of the large and moderate sized earthquakes occurred in the Marmara region. As such, the NW-SE trending fault segment translates the motion between the two E-W trending branches of the North Anatolian fault zone; one extending from the Gulf of Izmit towards C?narc?k basin and the other extending between offshore Bak?rkoy and Silivri.

The basic relation between the orientation of the maximum and minimum principal stress axes, the shear and normal stresses, and the orientation of a fault provides clue on the strength of a fault, i.e., its frictional coefficient. Here, the angle between the fault normal and maximum compressive stress axis is a key parameter where fault normal and fault parallel maximum compressive stress might be a necessary and sufficient condition for a creeping event. That relation also implies that when the trend of the sigma-1 axis is close to the strike of the fault the shear stress acting on the fault plane approaches zero. On the other hand, the ratio between the shear and normal stresses acting on a fault plane is proportional to the coefficient of frictional coefficient of the fault. Accordingly, the geometry between the Prince's islands fault segment and a maximum principal stress axis matches a weak fault model.

Keywords: stress tensor, fault orientation, frictional coefficient

Japan Geoscience Union Meeting 2015
(May 24th - 28th at Makuhari, Chiba, Japan)

SSS30-15 Room:A05 Time:May 25 14:30-14:45

High-frequency falloff exponent of source spectra: Case of Fukushima-Hamadori and northern Ibaraki area

UCHIDE, Takahiko[1*] ; IMANISHI, Kazutoshi[1]

[1]Geological Survey of Japan, AIST

The moment spectra, often referred to as the source spectra, have been investigated to characterize the earthquake source processes. The omega-square model has often worked as the standard model for the source spectra. The model has flat spectra in the lower frequencies and the falloff proportional to ω^{-2}, where ω is angular frequency, in the higher frequencies. The corner frequency dividing those two frequency bands represents the inverse of the source duration and therefore indicates the source size and then the representative stress drop.

The high-frequency falloff exponent is also an important source parameter. Although 2 of the exponent is often applicable, the exponent other than 2 is sometimes reported [e.g., Venkataraman et al., 2006; Allmann and Shearer, 2009]. Uchide et al. [SSJ Fall Meeting, 2014] found 1.6 of it in Hamadori (Coastal area) of Fukushima Prefecture and northern Ibaraki Prefecture, northeast Japan, by the stacking method [Shearer et al., 2006], while 2 worked well in the Tohoku-oki area, northeast Japan [Uchide et al., JGR, 2014]. This result must be confirmed by other method, therefore we here study the spectral ratio between target events and smaller events nearby (hereafter referred to as "empirical Green's function (EGF) event"), focusing on the high-frequency falloff exponent.

In order to stabilize the result, we obtain the spectral ratios using multiple time window [Imanishi and Ellsworth, 2006]. In addition, we stack the spectral ratios from multiple stations and all three components by taking the median spectral ratio at each frequency. Then we grid-search the high-frequency falloff exponent in addition to the corner frequencies of both the target and EGF events, and the seismic moment ratio of those events.

In fact, it is difficult to constrain the high-frequency falloff exponent from a single spectral ratio, since there is the trade-off between the corner frequency and the falloff exponent. Therefore we simultaneously fit the spectral ratios between the specific target and different EGF events, assuming the common corner frequency of the target event and the common falloff exponent for the target and EGF events. The preliminary result implies the high-frequency exponent less than 2.0 for some events, while some other events prefer 2.0 of the exponent. Finally we will discuss the cause of the variation in the high-frequency falloff exponent.

Keywords: earthquake, spectral study, spectral ratio

Japan Geoscience Union Meeting 2015
(May 24th - 28th at Makuhari, Chiba, Japan)

SSS30-16 Room:A05 Time:May 25 14:45-15:00

Earthquake cluster activity beneath Tanzawa Mountains in 2012: Migration with a small stress drop

YAMADA, Takuji[1*] ; YUKUTAKE, Yohei[2] ; TERAKAWA, Toshiko[3] ; ARAI, Ryuta[4]

[1]Inst. Seismol. and Volc., Hokkaido Univ., [2]Hot Springs Res. Inst. of Kanagawa Pref., [3]Earthq. and Volc. Res. Center, Nagoya Univ., [4]Japan Agency Marine-Earth Science and Technology

An earthquake cluster activity took place beneath the Tanzawa Mountains, which is located NE of Mt. Fuji, Japan, with a depth of 20 km at the end of January, 2012. The activity began at 22:39 UT on 27 January and included 78 earthquakes with M $\geq$ 2.0 in the area within 50 hours. Five of them had magnitudes greater than 4.0 and the largest one was M5.4.

First we relocated hypocenters by using the double difference method and found that earthquakes of the cluster activity migrated away from the first earthquake of the activity. The migration was consistent with the fluid diffusion and could be characterized as following two patterns. Earthquakes that occurred within an hour of the first earthquake had a migration speed similar to that of non-volcanic tremors. On the other hand, those occurred between an hour and 50 hours from the first earthquake of the activity showed a migration with a similar speed to the activity of induced earthquakes due to water-injection experiments. These results suggest that the cluster activity would be triggered by a slow slip and fluid diffusion. We confirmed that this migration would not be an apparent one by numerical simulations.

We then analyzed stress drops of 16 earthquakes with M $\geq$ 3.5 that occurred from July, 2003 to June, 2012 in the area of the activity. Earthquakes that occurred before and after the cluster activity had stable values of stress drop with 30 MPa estimated by the equation of Madariaga (1976), or 5 MPa by Brune (1970). On the other hand, earthquakes of the cluster activity included ones with significantly small stress drops. A hypothesis that the cluster activity was associated with fluid explains both the migration of hypocenters and small stress drops of the cluster activity. This is because the shear strength on a fault can be decreased due to the pore pressure of the fluid. This hypothesis is also supported by the fact that earthquakes before and after the cluster activity had similar values of stress drop and that structural studies indicated the existence of little fluid in the region, suggesting that the activity was triggered by a different mechanism from the other earthquakes in the same region. The most plausible explanation is that there is a little fluid in a closed system beneath the Tanzawa Mountains which is undetectable by structural observations.

Acknowledgments: We used waveforms at stations of Hi-net (NIED), Hot Spring Research Institute of Kanagawa Prefecture, Univ. of Tokyo, and JMA, as well as the seismograph network called the MeSO-net, which has been developed under the “Special Project for Earthquake Disaster Mitigation in the Tokyo Metropolitan Area” since 2007. We also used arrival times of P and S waves determined by JMA. Figures were created using Genetic Mapping Tool.

Keywords: Tanzawa Mountains, earthquake cluster activity, migration, stress drop, fluid, pore pressure

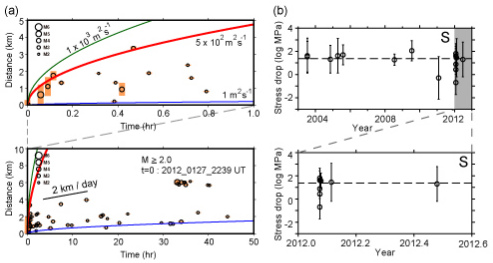

Fig. (a) Hypocentral distances from the first earthquake as a function of elapsed time less than an hour and 50 hours, with scales of source radii. Vertical orange bars indicate source dimensions calculated from estimated stress drops by S waves. Red curve with a diffusivity of 5.0 x 10^{2} m^{2} s^{-1} explains the data better than the other values (green and blue lines) for time < 1 hr. The seismicity for 1 ≤ time ≤ 50 hrs shows a migration with a speed of 2 km a day. (b) Estimated stress drops from S waves as a function of time. Black horizontal broked lines indicate average stress drops of earthquakes that occurred before and after the cluster activity. Results after January 2012 are also shown in the lower panel.

Japan Geoscience Union Meeting 2015
(May 24th - 28th at Makuhari, Chiba, Japan)

SSS30-17 Room:A05 Time:May 25 15:00-15:15

Resistivity structure and 3He/4He ratios around the focal zone of the 2011 Mw 5.9 earthquake beneath Mt. Fuji, Japan

AIZAWA, Koki[1*] ; SUMINO, Hirochika[2] ; UYESHIMA, Makoto[3] ; YAMAYA, Yusuke[4] ; HASE, Hideaki[5] ; OHNO, Masao[1] ; TAKAHASHI, Masaaki[4] ; KAZAHAYA, Kohei[4] ; RUNG-ARUNWAN, Tawat[6] ; OGAWA, Yasuo[7]

[1]Kyushu University, [2]Geochemical Research Center, Graduate School of Science, University of Tokyo, [3]ERI, University of Tokyo, [4]AIST, [5]GERD, [6]Mahidol University, [7]KSVO, TITECH

We present the results of a joint 3-D resistivity and isotopic analysis of the groundwater system surrounding Mt. Fuji, Japan, where increased seismicity was observed following the 2011 TohokuOki megathrust earthquake. The electrically conductive zone and high concentrations of magmatic helium correspond to this zone of triggered seismicity. In contrast, 2H (D) and 18O isotope ratios, and Li/Cl ratios do not support the presence of magmatic water. These results suggest that the earthquakes were triggered within a fractured zone where only magmatic gas preferentially travels upward. Although multiple mechanisms may jointly contribute to this remote earthquake generation, we hypothesize that a small fraction of gas bubbles, which are originally secured within the fracture zone by capillary trapping, play a key role for earthquake triggering.

Japan Geoscience Union Meeting 2015
(May 24th - 28th at Makuhari, Chiba, Japan)

SSS30-18 Room:A05 Time:May 25 15:15-15:30

Spatial variation of seismic radiation properties for large interplate earthquakes in northeast Japan

KUBO, Hisahiko[1*] ; IWATA, Tomotaka[2] ; ASANO, Kimiyuki[2] ; AOI, Shin[1]

[1]National Research Institute for Earth Science and Disaster Prevention, [2]Disaster Prevention Research Institute, Kyoto University

Kubo et al. (2014, AGU) constructed kinematic source models for the 2011 Tohoku-oki earthquake (M_w 9.1) in multi successive period-bands using strong-motion data, and discussed the period-dependent seismic radiation and broadband source characteristics for this event based on the spatial difference of the slip velocity function for each period-band. This multi period-band source modeling has an advantage that this method provides the direct comparison among source models in multi period-bands. In this study, we investigate the period-dependent seismic radiation for the 2011 Ibaraki-oki earthquake (M_w 7.9), which is the largest aftershock of the 2011 Tohoku-oki earthquake, using the same procedure as Kubo et al. (2014, AGU) in order to compare the rupture behaviors of these earthquakes and take the first step for the discussion on the spatial variation of seismic radiation properties for large interplate earthquakes in northeast Japan.

The analysis period-bands for the 2011 Ibaraki-oki earthquake is 5-10 s, 10-25 s, and 25-50 s. The source model for each period-band is estimated by the fully Bayesian kinematic source inversion with the multi-time-window method (Kubo et al., 2014, SSJ). Three components of strong-motion velocity waveforms at 15 stations of K-NET, KiK-net, and F-net of NIED are used in this analysis. Green's functions are calculated by the FDM (GMS; Aoi & Fujiwara, 1999) with a 3D velocity structure model (JIVSM; Koketsu et al., 2012). The validity of the 3D velocity structure model used for the 3D Green's functions was confirmed through waveform comparisons for M~6 events. A curved fault model is constructed based on the shape of the plate boundary of JIVSM, and then is divided into 144 subfaults of approximately 10 km $\times$ 10 km. The slip time history of each subfault is represented by a series of nine smoothed-ramp functions with 4.0 s width, each of which is put with 2.0 s lag. The first time-window triggering velocity of 2.0 km/s is selected so as to minimize the residual of strong-motion data fitting in the period-band of 5-50 s.

The estimated rupture process in the period-band of the 5-10 s differs from those estimated in the period-bands of 10-25 s and 25-50 s. The source models in period-bands of 10-25 s and 25-50 s have large slips in the shallow area south and southeast of the hypocenter, while large slips for the source model in the period-band of 5-10 s are located in the deep area which is approximately 30 km west of the hypocenter. This means that these regions mainly radiated the long-period (10-25 s and 25-50 s) and relatively-short-period (5-10 s) waves, respectively. These results indicate that the 2011 Ibaraki-oki earthquake had an along-dip variation in its seismic radiation, which is consistent with the along-dip segmentation of interplate fault suggested by Lay et al. (2012).

The comparison of the results for the 2011 Tohoku and the 2011 Ibaraki earthquakes indicates that the seismic radiation for both events was segmented along the dip direction: short- and long-period seismic waves were predominantly radiated from the deep and shallow regions, respectively. However, the deep off-Miyagi region during the 2011 Tohoku earthquake radiated not only short- but also long-period waves, and this implies the possibility of the spatial variation of seismic radiation property in northeast Japan. This is also supported by previous studies which have noted different seismic radiation properties among other large interplate earthquakes in the northeast Japan, although the details of the seismic radiation for the other earthquakes are not clear and it is necessary to apply the multi period-band source modeling to these events.

[Acknowledgments] The strong-motion data recorded by K-NET, KiK-net, and F-net of NIED was used for this analysis.

Keywords: Spatial variation of seismic radiation property, Large interplate earthquakes in northeast Japan, Multi period-band source modeling, Strong-motion data, The 2011 Tohoku-oki earthquake, The 2011 Ibaraki-oki earthquake

Japan Geoscience Union Meeting 2015
(May 24th - 28th at Makuhari, Chiba, Japan)

SSS30-19 Room:A05 Time:May 25 15:30-15:45

Randomness of megathrust earthquakes implied by rapid stress recovery after the 2011 Tohoku-oki earthquake

TORMANN, Thessa[1] ; ENESCU, Bogdan[2*] ; WOESSNER, Jochen[1] ; WIEMER, Stefan[1]

[1]ETH Zurich, Swiss, [2]Faculty of Life and Environmental Sciences, University of Tsukuba

Constraining the recurrence of megathrust earthquakes is genuinely important for hazard assessment and mitigation. The prevailing approach to model such events worldwide relies on the segmentation of the subduction zone and quasi-periodic recurrence due to constant tectonic loading. In this study, we have used the earthquake catalog of the Japan Meteorological Agency (JMA) and analyzed events recorded along a 1,000-km-long section of the subducting Pacific Plate beneath Japan since 1998 to map the relative frequency of small to large earthquakes, expressed by the slope of the frequency-magnitude distribution of earthquakes (the so-called b-value). Evidence from laboratory experiments, numerical modeling and natural seismicity indicates that the b-value is negatively correlated with the differential stress.

Our analysis reveals that the spatial distribution of b-values reflects well the tectonic processes accompanying plate motion. However, there is no evidence of distinct earthquake-generation regions along the megathrust, associated with the so-called ”characteristic earthquakes”.

Nevertheless, we show that parts of the plate interface that ruptured during the 2011 Tohoku-oki earthquake were highly stressed in the years leading up to the earthquake, as expressed by mapped, very low regional b-values. Although the stress was largely released during the 2011 rupture, thus leading to an increase in b-values immediately after the megathrust event, the stress levels (i.e., b-values) quickly recovered to pre-megaquake levels within just a few years. This suggests that the megathrust zone is likely ready for large earthquakes any time with a low but on average constant probability.

Our results imply that large earthquakes may not have a characteristic location, size or recurrence interval, and might therefore occur more randomly distributed in time. The findings also bring strong evidence that the size distribution of earthquakes is sensitive to stress variations and its careful monitoring can improve the seismic hazard assessment of the megathrust zone.

Reference:
Thessa Tormann, Bogdan Enescu, Jochen Woessner, Stefan Wiemer, Randomness of megathrust earthquakes implied by rapid stress recovery after the Japan earthquake, *Nature Geoscience*, **8**, 152-158, doi:10.1038/ngeo2343, 2015.

Keywords: Tohoku-oki earthquake, earthquake cycle, seismicity, b-value, differential stress

Japan Geoscience Union Meeting 2015
(May 24th - 28th at Makuhari, Chiba, Japan)

SSS30-20 Room:A05 Time:May 25 16:15-16:30

Radiated and Frictional Energy of the 2011 Tohoku-oki Earthquake

MORI, James[1*]

[1]Kyoto University DPRI

The Japan Trench Fast Drilling Project (JFAST) estimated the level of dynamic friction on the shallow portion of the fault that had the very large slip during the 2011 Tohoku-oki earthquake. From both laboratory experiments on the fault zone material and temperature measurements across the fault zone, the shear stress during the earthquake rupture was estimated to be about 0.6 MPa at 820 meters below the sea floor (including the water depth this is equivalent to about 3. 5 km of rock overburden). This shear stress corresponds to a coefficient of friction of about 0.1. Combining these results with estimates of the radiated energy, show that the ratio of frictional heat to radiated energy is less than 1.0 for the shallow portion of the fault. These estimates are related to the large slip portion of the earthquake in the shallow region of the megathrust and are not representative of the deeper portions of the earthquake rupture area. Averages for the whole earthquake suggest that the ratio of frictional heat to radiated energy is much larger (about 10) and similar to values inferred for typical earthquakes. This implies there is a significant difference in the energy partition between the shallow portion (with large slip) and the deeper portions (moderate slip) of the subduction fault. The shallow/deep portion of the fault produces relatively more/less radiated energy compared to the frictional heat.

Keywords: earthquake source, energy, Tohoku-oki earthquake, friction, radiated energy

Japan Geoscience Union Meeting 2015
(May 24th - 28th at Makuhari, Chiba, Japan)

SSS30-21 Room:A05 Time:May 25 16:30-16:45

Estimation of Radiated Seismic Energy of Repeating Earthquakes in Northeastern Japan and its Spatio-Temporal Variation

ARA, Masamichi[1*] ; IDE, Satoshi[1] ; UCHIDA, Naoki[2]

[1]The Univ. of Tokyo, [2]Tohoku University

Seismic activity on the plate interface is spatially heterogeneous. In addition to ordinary earthquakes of different sizes, tsunami earthquakes and slow earthquakes occur with much longer duration expected from the scaling relation of ordinary earthquakes. However, for example, the source areas of tsunami earthquakes are known to be located at shallower part of plate interface. Additionally, in the source area of the Tohoku-Oki earthquake, more high frequency seismic wave was radiated at deeper region of the plate interface [Ide et al., 2011]. Therefore, the fault property of the plate interface in the Tohoku-Oki region can be spatially heterogeneous. The spatial heterogeneity on the plate interface may result in the variation of radiated seismic energy, which conveys the information of dynamic rupture process. Among various earthquakes occurring near the plate interface, repeating earthquakes are relatively easy to understand because of its simple mechanism, as repeated slips of a small locked region of the plate interface to catch up with aseismic slip in surrounding region. Since, repeating earthquakes are considered to occur on the plate interface certainly, they are ideal targets to constrain the physical mechanism of brittle rupture on the plate interface. Many repeating earthquakes have been detected in the Tohoku-Oki region. The size and inter-event time of some repeating earthquake groups changed after the Tohoku-Oki earthquake. To examine the possible change of source process after the Tohoku-Oki earthquake can also contribute to the understanding of physical process of earthquakes. In this study, we estimated the radiated seismic energy of repeating earthquakes in the Tohoku-Oki region and examined its spatio-temporal variation.

The target earthquakes of this study are 160 repeating earthquakes detected by Uchida and Matsuzawa [2013]. These earthquakes are divided into 52 repeating earthquake groups. Seismic activity of these events extends before and after the Tohoku-Oki earthquake and includes groups that showed enlarged magnitude and shortened inter-event time after the earthquake as represented by Kamaishi sequence. To estimate radiated seismic energy, we use the method for measuring amplitude developed by Mayeda et al. [2003] and the method for estimating source spectra and radiated seismic energy developed by Baltay et al. [2010] with slight modifications. In this modification, we linearized the calculation to quantitatively estimate the error of the radiated seismic energy that has not been discussed precisely.

We obtained a positive depth dependency of scaled energy, the ratio between radiated seismic energy and seismic moment, as a main characteristic of spatial variation. This is consistent with the results in previous studies. We also observe some temporal changes in scaled energy. For Kamaishi-sequence, the scaled energy decreased suddenly after the Tohoku-Oki earthquake and gradually recovered, coinciding with a sudden increase and gradual decay of seismic moment. This temporal change of seismic moment has been interpreted as the expansion of rupture into conditionally stable region around the unstable region [Uchida et al., 2015]. The temporal change of scaled energy suggests that the ratio of fracture energy is larger in this conditionally stable region.

Radiated seismic energy is related to the strength of the fault, which increases after an earthquake. Therefore, we expect some correlation between the inter-event time and scaling energy for repeating earthquakes. In our result, there are several groups and regions that have positive dependency of scaled energy on the inter-event time, but this relation cannot be confirmed generally.

Japan Geoscience Union Meeting 2015
(May 24th - 28th at Makuhari, Chiba, Japan)

SSS30-22 Room:A05 Time:May 25 16:45-17:00

Emergence, moment change and disappearance of small repeating earthquakes following the 2011 Tohoku earthquake

HATAKEYAMA, Norishige[1*] ; UCHIDA, Naoki[1] ; MATSUZAWA, Toru[1]

[1]Graduate School of Science, Tohoku University

Small repeating earthquakes, which occur repeatedly at almost the same location, are thought to represent repeated ruptures of a small seismic patch on a fault plane. There are many unknown features about repeaters such as detailed structures of the patch and causes of irregularity in the magnitude and the recurrence interval.

Some small repeating earthquake sequences show systematically increased seismic moments after the 2004 M6.0 Parkfield earthquake (Chen et al., 2010) and the 2011 M9.0 Tohoku earthquake (Tohoku EQ; Uchida et al., 2015) in the areas where large afterslip occurred. These phenomena can be explained by increases in rupture areas due to aseismic-to-seismic transitions at high loading rate in conditionally stable regions around the repeaters. Understanding slip behavior changes in conditionally stable regions due to stress perturbation is important for revealing the generation mechanisms of recurrent interplate earthquakes.

In this study, we performed hypocenter relocations in a small area off Miyako-city, Iwate-prefecture, Japan, to examine temporal changes in seismic activities before and after the Tohoku EQ. We selected a small area including a cluster of earthquakes with repeaters at a depth of ∼40km, corresponding to the depth to the plate boundary. A large afterslip of the Tohoku EQ was estimated to have occurred in this area (e.g., Ozawa et al., 2012).

We used the double-difference method (Waldhauser and Ellsworth, 2000) for the hypocenter relocation. Firstly, we relocated events around the cluster by using pick-data of the Japan Meteorological Agency to select earthquakes in the cluster for further analysis. Secondly, we precisely relocated events in the cluster by using travel-time differences estimated from waveform cross-spectra.

The results show that before the Tohoku EQ, M2.5-2.9 events (Group A) repeatedly occurred at almost the same location with quasi-periodic recurrence intervals (9-12 months). There were no events whose magnitudes were larger than 2.0 within 5km from the repeaters.

After the Tohoku EQ, three significant changes were observed in the seismic activities in the cluster.

(1) At the location where the Group-A events had occurred before the Tohoku EQ, earthquakes larger than M3.0 started to occur repeatedly. The recurrence intervals were much shorter than before (eleven events from March to December 2011).

(2) In some areas where there had been no events before the Tohoku EQ, two repeating earthquake sequences appeared: M3.2-3.9 events (Group B) to the northwest of Group A and M2.2-4.4 events (Group C) to the northeast of the Group A. The centroids of the events in the Groups A-C were estimated to be located within 1 km.

(3) Magnitudes of the events in each group tended to become smaller as time passed. The Group-C events disappeared after the M2.2 event in January 1, 2012.

The phenomena similar to (1) were previously reported by Chen et al. (2010) and Uchida et al. (2015). These suggest that conditionally stable regions around the Group-A patch slipped seismically with the patch due to fast loading rate caused by afterslip of the Tohoku EQ. The phenomena in (2) can be interpreted as slip behavior changes in conditionally stable regions from aseismic to seismic due to the fast loading rate. The phenomena in (3) can be interpreted as that the rupture areas in the conditionally stable regions gradually shrunk over time as the loading rate decreased.

These results suggest that slip behavior changes that were probably dependent on the loading rate could cause not only changes in magnitudes but also emergence and disappearance of repeating earthquakes in some cases. These observations will be useful in the modeling of the plate boundary off Tohoku.

Acknowledgement: We used earthquake catalog and phase data produced by Japan Meteorological Agency. We also used waveform data from National Research Institute for Earth Science and Disaster Prevention, Hokkaido University and Hirosaki University.

Keywords: repeating earthquake, 2011 Tohoku earthquake, hypocenter relocation, conditionally stable region, afterslip

Japan Geoscience Union Meeting 2015
(May 24th - 28th at Makuhari, Chiba, Japan)

SSS30-23 Room:A05 Time:May 25 17:00-17:15

Early rupture process of the 14 March 2014 Iyo-Nada intermidiate-depth earthquake

SAITO, Mamoru[1] ; KOMATSU, Masanao[2*] ; TAKENAKA, Hiroshi[2]

[1]Okayama University, [2]Okayama University

An intermediate-depth earthquake (M_{JMA} 6.2) occurred in Iyo-Nada on March 14, 2014. The focal depth is 78 km, and this event occurred in the Philippine Sea slab. In this study, we investigate the early rupture process of this earthquake for about 5 seconds after the initial break. Three characteristic P-wave phases, P1, P2 and P3 are identified on the observed waveform records. Later phases has larger amplitude among the three phases. We estimate the generated position and time using the relative arrival time from the initial P phase for each of the three phases. We use vertical component of velocity waveform records at 52 seismic stations from the networks of JMA, NIED, AIST and Kyushu University, which are located at less than 105 km of epicentral distance, and read the arrival times and the polarities of the three phases and the first P arrival. Comparing the polarities of each arrival phase to the focal mechanism solution and the CMT solution from JMA, P1 phase corresponds to the focal mechanism, while P2 and P3 phases correspond to the CMT solution. Therefore, P1 phase is an initial rupture phase, while P2 and P3 phases are main rupture phases. The rupture position and time for each phase are estimated by the method of Takenaka *et al.* (2006, EPS) and its extension. As results, we found that initial P and P1 phases occurred on the east-dipping fault plane of the focal mechanism solution, while P2 and P3 occurred on north-dipping fault plane of the CMT solution. The two fault planes are crossover. The rupture moved from the initial rupture fault plane to the main rupture one. Focusing on the rupture times of the three phases, P1 phase was emitted by an event on the initial rupture fault plane at 0.49 seconds after the origin time of this earthquake. P2 phase then was generated by an event on the main rupture fault plane at 1.82 seconds after the origin time. P3 phase was emitted by a larger event at 3.3 seconds after the origin time.

Keywords: Rupture process, Initial rupture, Main rupture, Iyo-Nada

Japan Geoscience Union Meeting 2015
(May 24th - 28th at Makuhari, Chiba, Japan)

SSS30-24 Room:A05 Time:May 25 17:15-17:30

Evolution of rupture style with total fault displacement: insight from meter-scale direct shear experiments

XU, Shiqing[1*] ; FUKUYAMA, Eiichi[1] ; YAMASHITA, Futoshi[1] ; MIZOGUCHI, Kazuo[2] ; TAKIZAWA, Shigeru[3] ; KAWAKATA, Hironori[4]

[1]Nat'l Res. Inst. Earth Sci. Disas. Prev., [2]Centr. Res. Inst. Elect. Pow. Ind., [3]University of Tsukuba, [4]Ritsumeikan University

We report results with Indian metagabbro (Vs=3.62 km/s) that are obtained from a series of meter-scale direct shear experiments conducted at NIED. We focus on strain gage array data of stick-slip events loaded with 0.01 mm/s and under 6.7 MPa normal stress, and find the following: (1) During the early stage when the contact surface is relatively intact with less than 10 mm total displacement, ruptures mainly behave as slow-slip events (10 to 100 m/s). (2) With the accumulation of total fault displacement (up to several tens of mm), grooves indicative of strongly coupled local patches (i.e. asperities) are generated along the sliding surface, which are primarily elongated along the loading direction and are accompanied by notable gouge formation. The rest part of the surface continues being polished, indicated by a contrast in light reflectivity with respect to the initial level. At this stage, rupture speeds start to increase but are still well below the shear wave speed (˜1/4Vs). (3) After long enough total fault displacement (>500 mm), grooves and gouges of a sufficient amount are generated. The corresponding ruptures show, following a slow nucleation phase, fast propagation with speed comparable to the shear wave speed. Detailed strain data analysis shows that the above rupture style evolution is associated with an increasing efficiency in releasing the stored strain energy along the synthetic fault, which may have been facilitated by powder lubrication (Reches and Lockner, 2010) only after the formation of certain amount of gouges. Our study highlights the role of (evolving) fault surface properties in controlling propagation style of dynamic ruptures. It also calls for the need to conduct large-scale friction experiments over long displacement to better approximate natural fault conditions.

Keywords: Friction experiments, Dynamic rupture propagation, Fault lubrication

Japan Geoscience Union Meeting 2015
(May 24th - 28th at Makuhari, Chiba, Japan)

SSS30-25 Room:A05 Time:May 25 17:30-17:45

Cohesive Zone Length of Gabbro at Supershear Rupture Velocity (2)

FUKUYAMA, Eiichi[1*] ; XU, Shiqing[1] ; MIZOGUCHI, Kazuo[2] ; YAMASHITA, Futoshi[1]

[1]Nat'l Res. Inst. Earth Sci. Disas. Prev. (NIED), [2]Cntr. Res. Inst. Elect. Pow. Ind. (CRIEPI)

We investigated the shear strain field ahead of a supershear rupture. The strain array data along the sliding fault interfaces was obtained during large-scale biaxial friction experiments conducted at NIED in March 2013. These friction experiments were done using a pair of meter-scale metagabbro rock specimens whose simulated fault area was 1.5m x 0.1m. 2.6MPa normal stress was applied with loading velocity of 0.1mm/s. Along the fault edge parallel to the slip direction, 32 2-component semi-conductor strain gauges were installed at an interval of 50mm and 10mm off the fault. The data are conditioned by high frequency strain amplifiers (<0.5MHz) and continuously recorded at an interval of 1MHz with 16-bit resolution. Many stick-slip events were observed in this experiment. We chose unilateral rupture events in which foreshocks did not precede ahead of the main rupture and that propagated with supershear rupture velocity. One of the reasons for this selection was to improve the quality of observed data because the strain field ahead of the supershear rupture was not contaminated by elastic waves. Focusing on the rupture front, stress concentration was observed and sharp stress drop occurred immediately inside the rupture. We converted the temporal variation of strain to spatial variation of strain and picked up the peak strain and zero-crossing strain locations to measure the cohesive zone length. By compiling the stick-slip events, the cohesive zone length is 10 ˜20 mm. We could not see any systematic variation at the location but the cohesive zone length scattered between the events. We found that the cohesive zone length decreases with the total amount of slip as well as the rupture velocity increases, especially larger than root 2 times the shear wave velocity. This feature is more or less consistent with the theoretical prediction of Broberg (1999).

Keywords: cohesive zone, earthquake rupture, friction experiment, supershear rupture

Japan Geoscience Union Meeting 2015
(May 24th - 28th at Makuhari, Chiba, Japan)

SSS30-26 Room:A05 Time:May 25 17:45-18:00

Effects of plasticity on stick-slip behaviors of halite gouge

HIRAUCHI, Ken-ichi[1*] ; YOSHIDA, Yoshiaki[1] ; YABE, Yasuo[2] ; MUTO, Jun[3]

[1]Department of Geosciences, Graduate School of Science, Shizuoka University, [2]Graduate School of Science, Tohoku University, [3]Department of Earth Science, Graduate School of Science, Tohoku University

Non-volcanic tremors in subduction zones and San Andreas are known to be located near the bottom edge of the seismogenic zone. Assuming that the occurrence of ordinary earthquakes is inhibited by the onset of crystal plasticity in rock-forming minerals (e.g., quartz and feldspar), this implies that tremor activity occurs at the depth of a transition between brittle and ductile deformation. Previous studies of rock friction (Shimamoto, 1986, *Science*; Noda and Shimamoto, 2010, *GRL*) have already indicated that halite is a good candidate to explore the effects of plasticity on frictional behavior in laboratory, because with increasing normal stress (σ_n), the deformation mechanism of halite changes from frictional sliding to dislocation creep even at room temperature. However, it remains unclear how plasticity affects stick-slip behaviors of halite, including stress-drop magnitude, recurrence interval, frictional velocity dependence (a-b), and rupture propagation process.

To explore the effects of plasticity on stick-slip behavior, we conducted friction experiments on halite gouges at room temperature, constant normal stresses of 10 to 120 MPa, and sliding velocities of 1 or 10 μm/s, using a large biaxial testing machine installed at Tohoku University. Seven strain gauges were mounted on a forcing block at 23 mm intervals along the fault. For each experiment, we recorded more than 50 stick-slip events in total. At sliding velocity of 1 μm/s, the magnitude of stress drop increased from 1 MPa at σ_n = 10 MPa to 3 MPa at σ_n = 30 MPa, while decreasing to 0.5 MPa at σ_n = 120 MPa. The stick-slip recurrence interval at the same sliding velocity decreased from 20 s at σ_n = 10 MPa to 4 s at σ_n = 120 MPa. (a-b) values decreased from -0.005 at σ_n = 10 MPa to -0.025 at σ_n = 40 MPa, while remarkably increasing to 0.015 at σ_n = 120 MPa. Critical length (L_c) at which unstable, fast rupture propagation ($>$10% V_s) starts seems to increase with increasing σ_n.

Our experimental results indicate that the stick-slip behavior of halite fault gouges dramatically changes with increasing degree of plasticity, i.e., sharp, large stick-slip events in brittle regime evolve to smooth, small oscillations in semi-ductile (plastic) regime. Source characteristics of the small oscillations with sustained slow rupture may be linked to those of slow earthquakes such as non-volcanic tremors. It is well known that extremely low effective normal stress on the fault is the primary control on the occurrence of slow earthquakes. Furthermore, we suggest that the onset of plasticity in minerals, leading to an increase in (a-b), also facilitates the emergence of such slow transient creep events.

Keywords: friction experiments, halite, non-volcanic tremor, plasticity, rupture propagation, stick slip

Japan Geoscience Union Meeting 2015
(May 24th - 28th at Makuhari, Chiba, Japan)

SSS30-27 Room:A05 Time:May 26 09:00-09:15

Source Process of the 2014 ML5.5 Orkney earthquake, South Africa

OKUBO, Makoto[1*] ; CICHOWICZ, Artur[2] ; BIRCH, Denver[2] ; OGASAWARA, Hiroshi[3] ; MURAKAMI, Osamu[3] ; HORIUCHI, Shigeki[4]

[1]TRIES, ADEP, [2]Council for Geoscience, [3]Ritsumeikan Univ., [4]Home Seismometer Corp.

An earthquake occurred at 12:22:33 SAST (10:22:33 UT) on 5 August, with the epicenter near Orkney town near gold mines in the Klerksdorp district in the North West province of South Africa. The Council for Geoscience (CGS) in South Africa reported that the magnitude was M_L5.5. As a quick preliminary report, USGS estimated a left lateral fault mechanism and a focal depth of 5.0 km. CGS revised its depth to 4.7 km using the dense cluster network data. CGS also reported 84 aftershocks on 5 August and 31 aftershocks on 6 August, with magnitudes of 1.0 to 3.8 on the Richter scale. According to the CGS, this earthquake was the biggest recorded earthquake in the gold mining districts in South African history.

In this study, we analyzed the main shock waveforms and aftershock distribution to understand the rupture process of this earthquake. At the time of the 2014 Orkney earthquake, 17 strong motion surface stations were in operation and continuous acceleration seismograms were obtained with 24-bit and 200 Hz sampling. First, we picked P and S wave arrival times of the main shock and found two sets of phases in those seismograms. One belongs to a smaller event that occurred at a depth of 4.1 km (5.6 km below ground surface; BGS) with a magnitude less than 3. The other event started 0.3 seconds later with a larger magnitude slightly (1 km) north of the first one and at a depth of 4.2 km depth (5.7 km BGS). It seemed appears that the smaller initial rupture was leading led to a larger main rupture. According to the S wave velocity structure of in the Klerksdorp area, the S wave of the initial rupture can would have been able to reach to get to the hypocenter of the main rupture hypocenter, just in time. Thus, it seems that appears as though the initial rupture's S wave had initiated the main rupture.

Next, we applied hypoDD (Waldhauser & Ellsworth, 2000), the Double-Difference earthquake location algorithm, to P and S wave arrival times of the aftershocks, as well as to the initial and main ruptures of the main shock. We found spatial gaps in the deep parts of the aftershock distribution. These seem to correspond to the initial and main rupture hypocenters. We also found a horizontal seismic gap at a depth of 3.5 km BGS. Shallow events located above this seismic gap may have been caused by the M_L5.5 coseismic stress change and the existence of high mining rock stress. These might not be aftershocks since the gold mine leaf reaches up to a depth of 3.5 km.

According to Matsuda's law (Matsuda, 1975), the extent of a M_L5.5 earthquake fault can be 2-3 km (maximum for unidirectional rupture), main rupture could reach 2.5 km BGS. However, the existence of the horizontal seismicity gap and rupture extension at the same depth may imply that the main rupture did not reach 3.5 km BGS.

Keywords: SATREPS, initial rupture, Klerksdorp, double difference hypocenter location

Japan Geoscience Union Meeting 2015
(May 24th - 28th at Makuhari, Chiba, Japan)

SSS30-28 Room:A05 Time:May 26 09:15-09:30

Mitigation of the rockburst risk in deep South African gold mines

DURRHEIM, Raymond[1*] ; MILEV, Alexander[2] ; KGARUME, Thabang[2] ; BRINK, Van zyl[2] ; CICHOWICZ, Artur[3] ; OGASAWARA, Hiroshi[4]

[1]CSIR, South Africa, [2]University of the Witwatersrand, South Africa, [3]Council for Geoscience, South Africa, [4]Ritsumeikan University, Japan, [5]SATREPS

Earthquakes pose a significant risk to workers in deep and overstressed mines, such as South African gold mines. A 5-year collaborative project entitled OBSERVATIONAL STUDIES IN SOUTH AFRICAN MINES TO MITIGATE SEISMIC RISKS was launched in August 2010 to gain knowledge, develop and transfer technology, and build capacity. It was funded by the JST-JICA Science and Technology Research Partnership for Sustainable Development (SATREPS).

Rockbursts are seismic events that cause damage to underground workings. Strategies to mitigate the risk posed by rockbursts can be divided into three categories: prevention, protection and prediction. In this paper we will discuss the contribution made by the SATREPS project to these strategies.

Research sites were established at three deep gold mines: Cooke #4 Shaft, Hlanganani and Moab Khotsong. Boreholes were drilled to locate faults accurately that were considered capable of producing mining-induced seismic events. A variety of sensors were installed to monitor the quasi-static deformation of the rock mass, the accumulation of strain, tilt changes during the seismic event and post seismic creep phase, and changes in dynamic stress produced by the propagation of the rupture front. The Council for Geoscience (CGS) deployed 10 surface seismic stations in the Far West Rand district where the Cooke #4 and Hlanganani mines are situated. The CGS also manages a 25-station network established in the Klerksdorp district where the Moab-Khotsong mine is situated. SATREPS also provided a Kinemetrics Antelope Seismic Processing System to handle the large volume of data being acquired by the networks and the Horiuchi algorithm to automatically pick P- and S-arrival time and locate events.

By prevention, we mean a reduction in the occurrence of damaging seismic events. This is achieved by optimizing the design and sequence of extraction. Rock properties and the stress field are essential inputs. The SATREPS project has made a significant contribution to the mine design capability by adapting and transferring of the Compact Conical Borehole Overcoring (CCBO) stress measurement technique. Stress measurements, together with observations of borehole breakouts and discing of borehole core and seismic source parameters, are used to calibrate numerical models of mining layouts and sequences.

By protection, we mean the creation of rockburst-resistant excavations. As part of the SATREPS project we have studied the state of the rockwall in stopes near the research sites, measured the response of the rockmass to mining, and studied the performance of support elements and systems. In a complementary project, CSIR is developing various technologies to enable the stability of the hangingwall to be mapped prior to the entry of miners. These include robust closure and ground motion meters, thermal and acoustic mapping of hangingwall stability, and a robotic platform to carry these devices.

By prediction, we mean the reliable and timely forecasting of rockbursts so that mine workers may take refuge. We have used the unprecedented volume of high quality data gathered at the SATREPS sites to search for forerunners of seismic events. While we have gained new insights into the development of mining-induced fractures and the nucleation of seismic events, and studied variations in seismic parameters such as the b-value, we have not yet found a reliable precursory signal that can be used to raise an alarm.

Other lasting benefits of the SATREPS project include: (1) the enhancement of the National Seismograph Network, and (2) opportunities for several young South African researchers to visit Japanese institutes and gain experience in high-level research. The SATREPS project has been an extremely valuable contribution to researchers and practitioners working in deep South African mines, and we are grateful for the contributions of many dedicated Japanese scientists and the support of the Japanese government through JST and JICA.

Keywords: Mining induced seismicity, rockbursts, deep mines, South Africa, mitigation

Japan Geoscience Union Meeting 2015
(May 24th - 28th at Makuhari, Chiba, Japan)

SSS30-29 Room:A05 Time:May 26 09:30-09:45

Routine Estimation of Source Parameters of Mining-Related Earthquakes

CICHOWICZ, Artur[1*] ; BIRCH, Denver[1] ; MIYAKE, Hiroe[2] ; HORIUCHI, Shigeki[3] ; OGASAWARA, Hiroshi[4] ; DURRHEIM, Raymond[5] ; CGS, Technical team[6] ; THE SATREPS, Research group.[7]

[1]Council for Geoscience, South Africa / SATREPS, [2]The University of Tokyo, Japan / SATREPS, [3]Home Seismometer Corporation, Japan, [4]Ritsumeikan University, Japan / SATREPS, [5]University of the Witwatersrand and CSIR, South Africa / SATREPS, [6]Council for Geoscience, South Africa, [7]SATREPS (JST-JICA Science and Technology Research Partnership for Sustainable Development)

Mining in the Witwatersrand region of South Africa has led to induced seismicity. Seismicity is concentrated in several clusters associated with current mining production and flooding in abandoned mining voids. Starting in 2010, a surface network consisting of over 60 strong ground motion seismograph stations was installed in three clusters. Automatic earthquake location software from Home Seismometer Corp. based on an automatic location algorithm developed by Dr. Horiuchi was used to locate the large number of aftershocks quickly and accurately. Software for the estimation of seismic source spectral parameters was developed. The software is robust and most of the processing is performed automatically in a batch mode. A catalogue of a few thousand earthquakes was created and the spectral parameters of the events were estimated. Systematic shifts in the range of the spectral parameters for the three clusters were observed. Fluid-induced seismic events have a much smaller static stress drop (0.02- 5MPa) compared to areas where active mining is present (0.1-40MPa). The scalar seismic moment varied from 10^{10} to 10^{14} Nm for the fluid-induced seismicity cluster and for active mining it varied from 10^{10} to 10^{15} Nm. The relationships between static stress drop and scalar seismic moment undoubtedly show that the stress drop increases with seismic moment. Nevertheless, the scattering of the static or apparent stress drop around a fixed seismic moment spans roughly 1.5 -2.0 orders of magnitude.

An unexpectedly large earthquake of magnitude M_L 5.5 (M_w 5.3) was recorded in a district where active mining is currently taking place. Spectral analysis was performed in the frequency range 0.2 - 80Hz. An assumed quality factor of Q=400 was used. This value is used by underground mining networks. Kappa was set to 0.005. Analyzed waveforms were restricted to those recorded at small distances (2-20km) to reduce the effect of a possible error associated with the correction for path effects. The distribution of aftershocks located in the first 24 hours indicates the length of rupture zone to be roughly 6 km; however, spectral analysis of the entire S-wave group shows a maximum source size of approximately 2 km (S-wave corner frequency 1-1.3Hz). Visual inspection of the waveform clearly shows three sub-events. The first one is small followed by two stronger sub-events with similar pulse durations. The two strong sub-events occur about 0.5 sec apart. Analysis of the main event and aftershocks showed that the main event had a static stress drop of 35-45MPa, while the biggest aftershocks recorded in the first 10 days have static stress drops of 25-30MPa, and the largest aftershocks recorded in the next 10 days have static stress drops in the range 7-10MPa. The aftershocks with the largest static stress drops are distributed across the entire 6 km rupture zone. The relationship between stress drop and scalar seismic moment for all the aftershocks showed that the stress drop increases with seismic moment. The static stress drop varies in the range from 0.1 to 40MPa and scalar seismic moment varies from 10^{10} to 10^{14} Nm. The main event appears as a strong outlier with large scalar seismic moments of 2.6x10^{16} - 10^{17}Nm on the three components.

Keywords: spectral source parameters, induced seismicity, routine processing, static stress drop

Japan Geoscience Union Meeting 2015
(May 24th - 28th at Makuhari, Chiba, Japan)

SSS30-P01 Room:Convention Hall Time:May 25 18:15-19:30

Two seamounts in the near south of Nankai Trough concentrate stress like stake

MASE, Hirofumi[1*]

[1]none

(Please refer to the figure. Names of the slab, topography of seabed, etc are naming only of here.)

Collapse by intraplate earthquake, Separation of accretionary wedge, and Rotation of Slab by lateral-fault type are Nankai-Trough earthquakes. The role of the 2004 off Kii Peninsula earthquake is the settlement of the 1944 Tonankai earthquake (1). I want to search for the relation of both earthquakes further. I post almost clear points by (1)-(5).

(A):Concerning range of slip, it of 1944 did not reach the Trough, and it of 2004 twined round the Trough. Both are complementary and do not overlap so much.

(the following points are concerned in 2004)(B):The compression power in north-south is the cause.

(C):The foreshock, the main shock, and big aftershocks are distributed along the Trough, and are almost thrust-type that destroyed intraslab.

(D):Aftershocks distributed in northwest-southeast are almost shallow and lateral-type. In the accretionary wedge and the upper layer-of-lower-plate, the large-scale lateral fault belt exists.

(E):Everything is distributed in the west of the Crack(b).

(F):On the extension of the south end of the Crack(a), two big thrust-type aftershocks in 2 or 3 days occurred after the main shock.

(G):Large slip of the foreshock was in the deep place and in the vicinity of the hypocenter. That of the main shock was in the shallow place and in the west left from the hypocenter.(3) After all, the positions of both large slip are near.

About the large slip(G), there is Daiozaki Cape in almost due north and is WM Seamount in south. I think that the compression power(B) was the maximum in this north-south line. So that the power from the north that originates in the right-turning force(1) may concentrate in a narrow range in the vicinity of the Trough, existence like stake that concentrates the stress of reaction is dynamically indispensable in the south nearly of the Trough. WM Seamount might be ”Stake” exactly. EM Seamount where aftershock(F) occurred shortly in the vicinity might be ”Stake” too. The lateral fault belt(D) passes between two ”Stakes” in east and west.

The stress of WM Seamount that was large before the earthquake decreased sharply by the large slip(G). At this point, the north-south compression(B) has collapsed. Next, what happens? Because materials that exist in the left above of both ”Stake” in Fig.2 are alive and well, the stress from that direction(northwest) increases rapidly.

In a word in 2004, the north-south compression after 1944(B) might have been converted to the northwest-southeast compression in dramatic form. And, there is naturally a possibility of returning to the north-south compression(B) again in the future. Only this is the Tonankai earthquake when the future. Only this was the Tonankai earthquake in 1944.

(1)MASE(2014)/JpGU2014/SSS29-P10

(2)YAMANAKA(2004)/Source rupture processes of the 1944 Tonankai earthquake and the 1945 Mikawa earthquake/Chikyu Monthly/26/11/739-745

(3)YAGI(2004)/http://iisee.kenken.go.jp/staff/yagi/eq/Japan20040905/Japan20040905_1-j.html

(4)JMA/Monthly Report/September 2004

(5)KANAZAWA/http://cais.gsi.go.jp/YOCHIREN/history/2-3-6_kii2004.pdf

SSS30-P01 Room:Convention Hall Time:May 25 18:15-19:30

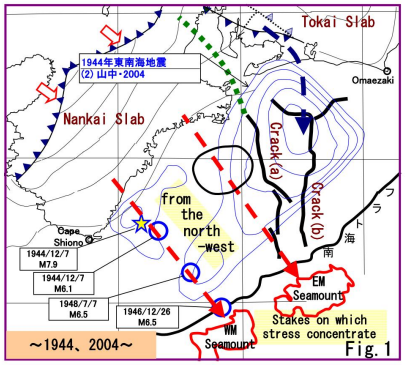

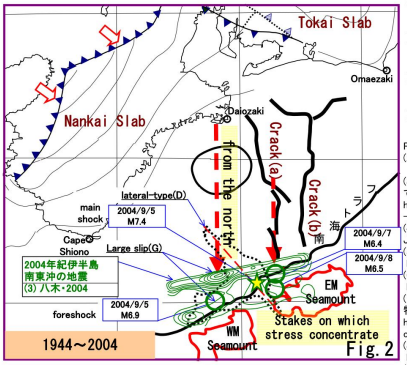

/About sea bottom
(shape line)
extracted from (6)/
/About "Nankai Slab"
(shape line, contour)
referable to (7)/
/About "Tokai Slab"
(shape line, contour)
referable to (8)/
/About information on earthquake
(All not mentioned specially)
referable to (9)/

Reference literature
(2)山中佳子(2004)/1944年東南海地震と1945年三河地震の震源過程
/月刊地球/26/11/739-745
(3)八木勇治(2004)/2004年9月5日紀伊半島南東沖で発生した地震について/建築研
http://iisee.kenken.go.jp/staff/yagi/eq/Japan20040905/Japan20040905_1-j.html
(4)JMA/Monthly Report on Earthquakes and Volcanoes in Japan/September 2004/特集2/図6-5(P64)等
(5)金沢敏彦/紀伊半島沖[三重県南東沖]の地震/東大震研
http://cais.gsi.go.jp/YOCHIREN/history/2-3-6_kii2004.pdf
(6)JHOD,JCG/Seafloor Topography of the Plate Boundaries
http://www1.kaiho.mlit.go.jp/jishin/sokuryo_E/sokuryo_E.html
(7)木村昌三(2001)/1946年南海地震に関係する四国における地震活動の特徴/(図2)
https://www.jstage.jst.go.jp/article/jgeography1889/110/4/110_4_581/_article/-char/ja/
(8)Nagoya Univ./Structure of the Subducting Philippine Sea Slab
http://www.seis.nagoya-u.ac.jp/SEIS/slab/slab-j.html
(9)JMA/Monthly Report on Earthquakes and Volcanoes in Japan/September 2004/特集2/図7-1(P65)
http://www.seisvol.kishou.go.jp/eq/gaikyo/index.html#monthly

Japan Geoscience Union Meeting 2015
(May 24th - 28th at Makuhari, Chiba, Japan)

SSS30-P02 Room:Convention Hall Time:May 25 18:15-19:30

Toward rapid source process analysis for great earthquake using teleseismic body waves

YOSHIMOTO, Masahiro[1*] ; YAMANAKA, Yoshiko[1]

[1]Environmental studies, Nagoya University

Source processes for great earthquakes are now obtained in near-real-time by teleseismic body wave analyses. Green's functions of most teleseismic body waves analyses are based on ray theoretical method, but such methods have the following two problems for great earthquakes source process analyses: difficulty in calculating all later phases such as PP waves and impossibility of calculating very long period phase called a W phase. To solve these problems, we introduced the complete Green's functions (i.e., all body and surface waves) calculated by Direct Solution Method. We show that source process analyses results of 2011 Tohoku-Oki earthquake (Mw7.3), 2007 Solomon earthquake (Mw8.1), and 2010 Chile earthquake (Mw8.8) using the complete Green's functions. We also analyzed these earthquakes using the conventional ray theoretical Green's functions in order to make clear the problems of ray theoretical method. The obtained 2011 Tohoku-Oki earthquake source process using complete Green's functions is not so different from ray theoretical Green's functions. However, the source process of 2007 Solomon and 2010 Chile earthquake using conventional ray theoretical Green's functions are quite different especially later part of source process compared with that of using the complete Green's functions. These difference mainly caused by neglecting W phase of the ray theoretical Green's functions calculation. When you analyze the great earthquake in near-real-time using ray theoretical Green's functions, we recommend that you should be use the station of small amplitude W phase as much as possible and may be better use velocity observed seismograms rather than displacement observed seismograms.

Keywords: teleseismic body waves, Green's functions, ray theory, W phase, great earthquake

Japan Geoscience Union Meeting 2015
(May 24th - 28th at Makuhari, Chiba, Japan)

SSS30-P03 Room:Convention Hall Time:May 25 18:15-19:30

Optimization of Preset Parameters for Source Process Analysis with Teleseismic Body-Wave

FUJITA, Kenichi[1*] ; KATSUMATA, Akio[1] ; SAKODA, Koji[2] ; SHIMIZU, Jumpei[2] ; HASEGAWA, Yoshiomi[2]

[1]Meteorological Research Institute, [2]Japan Meteorological Agency

1. INTRODUCTION

The Japan Meteorological Agency (JMA) analyzes source process of earthquakes in the world larger than Mw7.0 with teleseismic body-wave. The results are published on the website. It is generally difficult to determine optimum preset parameters for source process analysis, because there are so many parameters for the analysis. Therefore, it takes a long time until publish the results.

We examined optimized preset parameters to automate source process analysis with teleseismic body-wave. Here, we analyze some events using parameters which are determined automatically, and compare them with the results which were analyzed through trial and error by the analyst. Then, we extract problems which arises in automatic parameter determination and seek the solutions.

2. Methods

We use the same program package as Iwakiri et al. (2014) for analyzing source process with teleseismic body-wave. We use broadband waveform data which are downloaded from IRIS DMC HP, and apply band-pass filter (from 0.002Hz to 0.125Hz) to them. We use epicenter data of JMA for events in and around Japan, we use epicenter data of USGS for events in other areas. We use depth of CMT solutions of JMA for the depth of starting point. Hypocenter is set at center of assumed fault plane, and subfault parameters (size and number) are set by scaling law. Strike, dip and rake parameters are set from CMT solutions of JMA. Velocity structure for Green's functions are set based on the IASP91 model, and CRUST2.0 model for near hypocenter. Source-time functions are set with triangle functions. The number of function is changed based on event magnitude. And rise time is set at 2.0sec. We use ABIC (Akaike (1980)) for temporal and spatial smoothing constraints, and set hyperparameters as ABIC value become the minimum. Max rupture speed is set at 0.72 times of S-wave velocity from empirical relationship of Geller (1976).

Keywords: source process, optimized preset parameters, automation

Japan Geoscience Union Meeting 2015
(May 24th - 28th at Makuhari, Chiba, Japan)

SSS30-P04 Room:Convention Hall Time:May 25 18:15-19:30

Consideration of the Method to Estimate the Radiated Seismic Energy from Regional Seismic Waveforms

KIUCHI, Ryota[1*] ; MORI, James[1]

[1]DPRI, Kyoto University

The total released strain energy during an earthquake is divided into frictional energy, fracture energy, and radiated seismic energy. In these 3 components, we can estimate only the radiated seismic energy directly from the seismic waveform, and that characterizes the dynamic source property. There are large variations of radiated seismic energy from previous energy estimate studies, although it is difficult to estimate it due to the contribution from a wide frequency spectrum. One of the probable factors of this variation is focal mechanism dependence of radiated seismic energy from teleseismic waveforms (e.g., Choy and Boatwright, 1995; Convers and Newman, 2011). However, there are 2 additional questions from these studies. 1. These results were obtained only from P wave energy assuming a ratio between P wave energy and S wave energy. Teleseimic S waves often overlap with other phases, and attenuate more strongly than P waves, so it is difficult to measure the S-wave energy directly. The ratio of P to S radiated energy is not well known. 2. The focal mechanism dependence has been shown only for large earthquakes (Mw >6), it seems that this characteristic has not been observed for small and moderate earthquakes.

For the purpose of investigating these questions, we need to estimate and compare the radiated seismic energies correctly from several different phases. As an example, we focus on a moderate earthquake (June 14, 2008 at 12:27, Mw 4.9 from F-net) that occurred just after 2008 Iwate-Miyagi Nairiku earthquake. In this study we estimate the radiated seismic energy from regional P waves, S waves, and S wave coda using an empirical Green's function (EGF) method. The regional waveform data are recorded at stations of Hi-net. Firstly, using cross correlation, we select an EGF event that is highly correlated with the target event. Secondly, we deconvolve the seismograms in frequency domain with a multitaper method (Prieto et al., 2009), and check the waveform in time domain. Thirdly, we fit the obtained spectrum to an omega square model (Brune, 1970, 1971) to estimate the corner frequency. In addition, we try to vary the value of the power for the high-frequency fall-off. Finally, we calculate the radiated seismic energy using these spectra.

Acknowledgement
The regional waveform data of Hi-net and focal mechanisms of F-net were provided by NIED.

Keywords: Seismic radiated energy, Moderate earthquake

Japan Geoscience Union Meeting 2015
(May 24th - 28th at Makuhari, Chiba, Japan)

SSS30-P05 Room:Convention Hall Time:May 25 18:15-19:30

Simulation of hypocenter determination by using S-net stations

SHIMBO, Takashi[1*] ; UEHIRA, Kenji[1] ; KANAZAWA, Toshihiko[1] ; MOCHIZUKI, Masashi[1] ; FUJIMOTO, Hiromi[1] ; NOGUCHI, Shin-ichi[1] ; KUNUGI, Takashi[1] ; SHIOMI, Katsuhiko[1] ; AOI, Shin[1] ; SEKIGUCHI, Shoji[1] ; MATSUMOTO, Takumi[1] ; OKADA, Yoshimitsu[1] ; SHINOHARA, Masanao[2] ; YAMADA, Tomoaki[2]

[1]NIED, [2]ERI

To observe earthquakes occurring under seafloor and tsunami, project to construct Seafloor Observation Network for Earthquakes and Tsunamis along the Japan Trench (S-net) is started in 2011. The S-net consists of 150 seismic and tsunami observation stations. These stations are arrayed from off Hokkaido to off Boso at intervals of about 30km in the direction North-South (parallel to the trench axis) and at interval of about 50-60km in the direction East-West (perpendicular to the trench axis). S-net makes it possible to forecast earthquake warning and tsunami warning much earlier than presence. To understand occurrence of earthquake occurring under seafloor, we must research hypocenters distribution, focal mechanism, velocity structure, and stress field under seafloor accurately. Then we need to research relationship between subducting plate and occurrence of earthquake and process of strain accumulation at interplate. To research these in detail, we need to locate hypocenters under seafloor precisely.

To understand accuracy of hypocenters determined by S-net, we simulated of hypocenter determination by using travel times from earthquake occurring under seafloor to stations of S-net. 99 aftershocks at the southern region of 2011 off Pacific Cast of Tohoku Earthquake located by pop-up ocean bottom seismometers (OBSs) (Shinohara et al., 2011) were used. We calculated travel times from these hypocenters to S-net stations and estimated arrival times of every station. Hypocenters were determined by using the arrival times. Then velocity structure used calculation of travel times and determination of hypocenters was modeled by introducing result of seismic survey for installation of S-net. We compared hypocenters located by simulation of this study with those located by OBS data (Shinohara et al., 2011). As the result, difference in the hypocenters was about 1km. We run same simulation by using Hi-net land stations. Then velocity structure used calculation of travel times and relocation of hypocenters was velocity model used determination of hypocenter in Kanto and Tokai area (Ukawa et al., 1984). As the result, several hypocenters by simulation of this study were determined 5km deeper than those by OBS. This indicates that determination of hypocenter using only land seismic stations is not sufficiently precise.

Japan Geoscience Union Meeting 2015
(May 24th - 28th at Makuhari, Chiba, Japan)

SSS30-P06 Room:Convention Hall Time:May 25 18:15-19:30

The M 7.7 September 24, 2013 Pakistan earthquake: comparison of back-projection images and field data

WANG, Dun[1*] ; MORI, James[2] ; KAWAKATSU, Hitoshi[1]

[1]Earthquake Research Institute, The University of Tokyo, [2]Disaster Prevention Research Institute, Kyoto University

We analyzed the 24 September 2013 Pakistan earthquake (Mw 7.7) by back-projecting seismograms recorded by several large regional arrays in Japan, China, and Europe. The results show that the rupture propagated towards the southwest, and released most of the high frequency energy at 90-130 km southwest of the epicenter around 20-40 s after the initiation. This rupture pattern is significantly different from the northward propagation which would have been expected from the aftershock distribution.

High frequency images suggest that the average rupture speed is 4.0 to 5.0 km/s. The rupture speed seems relatively slow (1.0 to 2.0 km/s) for the first 10-15s, and then increased to fast, possibly supershear (4.0 to 6.0 km/s). Relatively lower frequency images show a lower rupture speed of 3.0 to 3.5 km/s (Figure 1).

A comparison of rupture traces determined by the back-projection and a geodetic study provides a good test for resolution of the back-projection method. Given a correct epicenter location, results derived from seismograms recorded in Hi-net, show a very accurate location of the surface trace with an uncertainty of 10-20 km.

Figure caption

Figure 1 Timings and amplitudes for the stack with the maximum correlation at each time step (1 s) showing in the map (top) and as a function of time derived from data recorded in Europe, China, and Japan (from left to right) filtered in several high frequency bands (bottom). Here the distance is measured in a straight line from the relocated epicenter.

Keywords: source process, back-projection, slip model, rupture speed

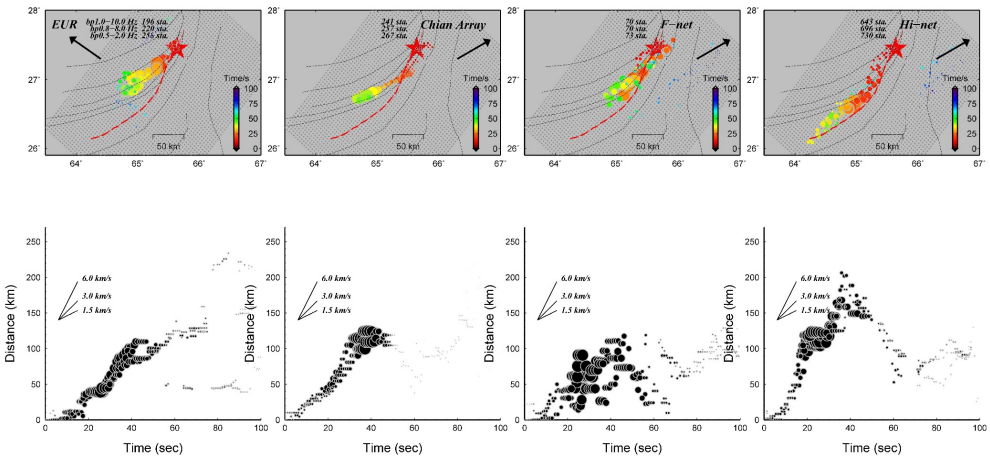

Japan Geoscience Union Meeting 2015
(May 24th - 28th at Makuhari, Chiba, Japan)

SSS30-P07 Room:Convention Hall Time:May 25 18:15-19:30

Source process analysis of the 1923 Kanto earthquake using 3-D Green's functions and a curved fault model

YUN, Sunhe[1*] ; KOKETSU, Kazuki[2] ; KOBAYASHI, Reiji[3]

[1]Earthquake Research Institute,The University of Tokyo/Itochu techno-solutions, [2]Earthquake Research Institute,The University of Tokyo, [3]Graduate School of Science and Engineering, Kagoshima University

The Kanto earthquake occurred on September 1, 1923 (UTC). The source region included the land area, causing severe damage in the Kanto district. This is an inter-plate earthquake along the Sagami trough. Large seismic intensities were observed not only around the source region but also in areas far from there. This strange distribution was caused by a 3-D complex structure of the Kanto basin. We calculated Green's functions using a Japan integrated velocity structure model by Koketsu et al. (2008) to include effects of the Kanto basin on ground motions and we performed source process inversions of the Kanto earthquake. This model reflects a 3-D complex shape of the Kanto basin and sedimentary layers are more than 3 km under the Tokyo bay and the northern Chiba prefecture. The dataset consists of static displacement, teleseismic, and strong motion data. We adopted both the same fault model as used by Sato et al. (2005) and a curved fault model. For the latter model we reconfigured the depths following the plate boundary.

We first calculated Green's functions using a half-space medium, a 1-D and a 3-D velocity structure model. The 3-D Green's functions are larger and longer than others and amplified later phases are remarkable. This means soft and 3-D complex sedimentary layers amplify Green's functions. We performed source process inversions using these Green's functions and geodetic data. All results show the similar large slip areas. But the total seismic moment of the result using 3-D Green's functions is the smallest. This implies amplifications by the basin also affect source process inversion results of only geodetic data. Next we used 3-D Green's functions and performed a joint inversion of static displacement, teleseismic, and strong motion data with the plane fault model. The large slip areas are similar to the result of Sato et al. (2005) but our result shows smaller slips and a smaller total seismic moment. In addition, we could obtain inversion results that provide good agreement in the later parts of the strong motions. We finally used 3-D Green's functions and performed a joint inversion with the curved fault model. The results show the western large slip area is moved to the southwest on the shallow part of the plate boundary, where is far from the hypocenter. Our result with the curved fault model shows larger slips and a larger total seismic moment than our result with the plain fault model. This is because the depths of the curved fault model are deeper, so Green's functions are smaller.

The results by the plane fault model and Sato et al. (2005) obtained the western large slip area where many aftershocks occurred. But our result with the curved fault model obtained the western large slip area where relatively a few aftershocks occurred. This is coincident with previous researches about the relationship between slip distributions and aftershock distributions. On the other hand, both the results with the plane and curved fault models show similar rupture propagations. The rupture started at a protruded area on the plate boundary and propagated to shallow southern parts for the initial 20 s. Then the rupture propagated to eastern areas where the plate boundary is dented for the next 20 s.

This study indicates that a velocity structure should affect not only strong motions but also static displacements for earthquakes occurred beneath the Kanto basin, which has thick sedimentary layers and a 3-D complex velocity structure. As a result, source process inversion results using a half-space and 1-D velocity structure models may overestimate slips and total seismic moments. In addition, we could obtain inversion results that provide good agreement with strong motions. This indicates the significance of using 3-D Green's functions in source process inversions. And the result with the curved fault model shows the slip distribution agrees with the established theory on aftershock patterns and a main shock faulting.

Keywords: source process inversion, 3-D Green's function, Kanto basin

Japan Geoscience Union Meeting 2015
(May 24th - 28th at Makuhari, Chiba, Japan)

SSS30-P08 Room:Convention Hall Time:May 25 18:15-19:30

Reproduction of M˜2 earthquakes by elastic Boundary Element modelling and constraint of Mohr-Coulomb failure criterion

UCHIURA, Taka[1*] ; HOFMANN, Gerhard[2] ; WIGGINS, Mitch[3] ; STONE, Wouter[3] ; NDABA, Pinkie[3] ; PLOTZ, Janelle[3] ; LENEGAN, Patrick[3] ; YILMAZ, Halil[4] ; ZVARIVADZA, Tawanda[4] ; MNGADI, Siyanda[4] ; CARPEDE, Andrew[4] ; DURRHEIM, Raymond[5] ; MILEV, Alexv[6] ; OGASAWARA, Hiroshi[7] ; YABE, Yasuo[8] ; KATO, Harumi[9]

[1]Ritsumeikan University, [2]Anglogold Ashanti, [3]Sibanye Gold, [4]Witwatersrand University, [5]CSIR / Witwatersrand University / SATREPS, [6]CSIR, [7]Ritsumeikan University / SATREPS, [8]Tohoku University / SATREPS, [9]3D Geoscience, Inc.

Several M˜2 earthquakes have taken place at a mine, close to one of the sites of the JST-JICA SATREPS project. At this site, three Ishii borehole strainmeters were installed, continuously monitoring at a sampling frequency of 100Hz since December 2011 and achieving better data return than previous projects. Although an AE network was not planned at this site, CSIR installed four 14Hz geophones with spatial intervals less than 100m to improve hypocenter location accuracy of the in-mine seismic network (station intervals $>$˜500m yielding a few ten of meters of errors in epicenter locations and much larger errors in z-location). The initial stress assumption was well calibrated at the adjacent mine (˜3 km to the west; Hofmann et al., 2013) and in-situ stress measurements ˜1km to the south in a mine are available. Uniaxial laboratory tests were conducted to measure elastic and strength properties of selected core collected from the nine holes with a total length of about 340 m for the instrumentation,.

This study attempted to numerically simulate four M˜2 earthquakes (one and the next occurred in December 2013 and January 2014 respectively and the remaining two in August 2014) that occurred in a range of distances from 180m to 351 m from the site by using an elastic Boundary Element stress modelling software, Map3D. In Map3D stress modelling, non-linear elasto-plastic fault ride is reproduced with its magnitude and extent controlled by the peak and residual strength, when estimated stress reaches specified peak strength.

Hofmann et al. (2012) successfully reproduced plausible source size and mechanism of an Mw2.2 event which had occurred at a dyke at Mponeng mine in December 2007. They took into account the aftershock planer cluster Yabe et al. (2009) delineated by the JAGUARS AE network (Nakatani et al., 2008). Hofmann et al. found that the aftershock plane coincided with that plane with largest Excess Shear Stress (i.e. shear stress exceeding shear strength; ESS). It could therefore be suggested that we could define slip planes with some confidence if we find planes with maximum ESS.

In this study, progressive tabular mining about 1m thick was modelled on a mine-wide scale by Displacement Discontinuity planes that represented the monthly advance of mining faces from December 2012 to August 2014. We used the initial stress state determined by Hofmann et al. (2013) and calibrated with several in-situ stress measurements in adjacent mines several km to the west of a mine. We also confirmed the assumed initial stress could reproduce stress states capable of producing breakout or core-discing that was actually observed in nine instrumental holes at our site. In the stress states just prior to the occurrence of the four M˜2 events, we grid-searched (in 10 degree increments of dip) for the plane with maximum ESS that contained the located hypocenter and had a strike parallel to the edge of the closest thin tabular stope. We found that for three of the four M˜2 event, composite plots of shear stress versus normal stress on assumed fault planes were relatively well limited by a single Mohr-Coulomb strength criterion line, but the strength suggested was significantly larger than those suggested by Hofmann et al. (2012), while the strength suggested for the remaining event were similar to that estimated by Hofmann et al. (2012). We have to discuss potential reasons, e.g., alteration of stress field by some geological structures or difference between intact rock and existing plane of weakness. The progress in the discussion, including analyses of the monitored strain change, will be reported in 2015 JpGU meeting.

Keywords: Mohr-Coulomb failure criterion, Deep South African mines, Elastic Boundary Element modelling, Stress in seismogenic zone

Japan Geoscience Union Meeting 2015
(May 24th - 28th at Makuhari, Chiba, Japan)

SSS30-P09 Room:Convention Hall Time:May 25 18:15-19:30

Detection state of stress at a fault from focal mechanism data ? application to Kego fault-

MATSUMOTO, Satoshi[1*] ; MIYAZAKI, Masahiro[1] ; SHIMIZU, Hiroshi[1]

[1]Institute of Seismology and Volcanology, Kyushu Univ.

One of the approaches used to evaluate the potential of an earthquake occurrence is the detection of the stress concentration at an earthquake fault. The stress fields for pre- and post-seismic event stages differ. However, this change cannot provide information regarding the potential for an earthquake to occur. Matsumoto et al. (2014) have proposed a detection method for states of stress that uses focal mechanism data of microearthquakes. The state of stress in this study can be defined by a moment tensor equivalent to the stress concentration normalized by differential stress. We apply this method to actual focal mechanism data from the 2005 Fukuoka earthquake and around the Kego fault, Kyushu, Japan, and discuss the presence of stress concentration around the earthquake fault before the mainshock.

Keywords: stress field, state of stress, focal mechanism, Kego fault

Japan Geoscience Union Meeting 2015
(May 24th - 28th at Makuhari, Chiba, Japan)

SSS30-P10 Room:Convention Hall Time:May 25 18:15-19:30

Estimates of stress drop in the focal area of the 2008 Iwate-Miyagi nairiku earthquake

YOSHIDA, Keisuke[1*] ; HASEGAWA, Akira[2] ; OKADA, Tomomi[2] ; UCHIDA, Naoki[2]

[1]National Research Institute for Earth Science and Disaster Prevention, [2]Tohoku University

Earthquakes release the deviatoric stress in the earth by slip on faults. We can estimate the magnitudes of the shear stress reductions (stress drops) on the faults through frequency analysis of seismic wave. Stress drop is an important parameter in earthquake cycle. However, it is generally difficult to accurately determine the stress drop. This is because it depends on many assumptions, and the estimates are largely affected by the errors of the corner frequency. Therefore, meanings of stress drop variations are not well understood. One possibility is that stress drops may related to frictional strengths on the fault planes. Determinations of absolute frictional strengths are very difficult. However, we can estimate the relative strengths from fault plane orientations of focal mechanisms in homogeneous stress regions. In this study, we investigate the relationship between stress drop and frictional strength. For that, we apply a multi-window spectral ratio method of Imanishi and Ellsworth [2006] to data from the dense aftershock observation network in the aftershock area of the 2008 Iwate-Miyagi nairiku earthquake. In the focal area, the stress orientations were estimated by Yoshida et al. [2014a and b]. Furthermore, the deviatoric stress tensors in the focal area were also estimated based on the rotations of principal stress axis after the mainshock [Yoshida et al., 2014b].

We estimated stress drops for earthquakes listed in JMA catalogue with magnitudes greater than 1.0. First, velocity spectrums of S-wave were calculated for three time windows, whose lengths are 2s moving in steps of 1s from 0.2s before the S-wave arrivals. Also, the velocity spectrums of noise were computed from time windows before the P-wave arrivals. We omitted data with S/N $<$5.0 near their expected corner frequencies. Second, spectral ratios were calculated between events within 1 km. For the hypocenters, we adopted those determined by double-difference methods to arrival time data from the temporary stations above the focal area [Yoshida et al.,2014b]. Third, corner frequencies were estimated by fitting the stacked spectral ratios with omega-square source model by Boatwright [1978]. Again, we omitted the results for which we could not constrain the corner frequencies enough due to high residuals. Finally, we estimated the stress drops using the circular crack model of Sato and Hirasawa [1973] and Eshelby [1957].

The number of estimated stress drops was 761. The mean and median values are 5.1 and 4.5 MPa, respectively. Although estimated values of them scatter, we found a positive correlation between the stress drop and the focal depth. For comparisons with frictional strengths, we estimated the relative frictional strengths based on the four stress orientations estimated by Yoshida et al. [2014a and b] in various spatial scales. For the estimations, we assumed the uniform differential stress magnitude within the focal area. In all cases, we see the positive correlation between the stress drops and the relative frictional strengths. In addition, we compared the results with the absolute frictional strengths estimated by Yoshida et al. [2014b] based on the spatially variable deviatoric stress tensors. Again, we found a positive correlation of the stress drops with the frictional strengths. These suggest that static stress drop released by earthquakes is related to the absolute stress level on fault plane.

Keywords: stress drop, stress tensor inversion, frictional strength, focal mechanism

Japan Geoscience Union Meeting 2015
(May 24th - 28th at Makuhari, Chiba, Japan)

SSS30-P11 Room:Convention Hall Time:May 25 18:15-19:30

Deep tremors response to tidal stress in western Japan: Analysis by Schuster's test

KIKUCHI, Junji[1*] ; YABE, Suguru[1] ; IDE, Satoshi[1] ; TANAKA, Yoshiyuki[2]

[1]Department of Earth and Planetary Scinence, The University of Tokyo, [2]Earthquake Reserch Institute, The University of Tokyo

In Japan, many deep tectonic tremors occur in the Nankai subduction zone from the center of Honshu to western Shikoku. Each tremor is a tiny shear slip that reflects local plate motion. Thus the physical conditions that enhance tremor activity would also control plate motion to some extent. For example, in a small tremor cluster beneath south Okayama, tremor rate is extremely well correlated with tidal level [Ide & Tanaka, 2014]. Here, we calculate ocean and solid earth tidal stress on the plate interface and quantitatively evaluate the degree of tidal triggering of tremors in the Shikoku region using the Schuster's test [e.g., Tsuruoka et al.,1995].

In the Shikoku region, we calculate normal and shear stresses at each reference point located at 0.1^o interval at 30 km depth, assuming a low-angle thrust fault based on global subducting plate motion. We compute the spatial distribution of theoretical ocean height using NAO.99b [Matsumoto et al., 2000] and convolve it with Green's function [Okubo & Tsuji, 2000] to obtain an ocean tidal stress tensor. We also calculate a stress tensor by solid earth tide using tide-generating potential of Tamura [1987]. The tremor catalog is of Idehara et al. [2014], for the nine years period from April 1, 2004 to March 31, 2013. We use tremors within $\pm 0.1^o$ in latitude and longitude, respectively, from each reference point.

In the Schuster's test, a phase angle of 0^o is assigned to the maximum stress peak nearest to the tremor occurrence time and $\pm 180^o$ to the following and preceding minima respectively. Based on the phase angles of all tremors, we calculate the significance level p for rejecting the null hypothesis that tremors occur randomly, regardless of stress. In general, small p means large statistical significance, and p less than 1% is considered significant in many previous studies.

We found some spatial variation in tremors response to tide. For example, in Kagawa, we found that two tremor clusters of similar sizes separated by 20km differently respond to tidal stress. The western cluster shows a strong tidal dependency (p=7.6e-44%), while eastern cluster has two peaks in phase angle and its tidal dependency is obscure. By changing fault parameters for the east cluster, we found that a low p (=0.7%) and a single peak in phase angle are obtained with some mechanisms similar to strike slip. This result implies that fault structure in Eastern Shikoku is complex and that tremor occurring mechanism changes locally.

Keywords: deep tectonic tremors, tide, Schuster's test, Nankai Trough, Shikoku

Japan Geoscience Union Meeting 2015
(May 24th - 28th at Makuhari, Chiba, Japan)

SSS30-P12 Room:Convention Hall Time:May 25 18:15-19:30

Seismicity Activation around the Kurobe Dam Reservoir in Oct. 2011

SATO, Takanobu[1*] ; KIM, Ahyi[1] ; OHMI, Shiro[2]

[1]Yokohama City University, [2]Disaster Prevention Research Institute, Kyoto University

After the March 2011 Tohoku-Oki earthquake, seismicity activation was observed wide range of beneath the Hida mountain area. However, another significant seismicity occurred around the Kurobe dam reservoir in October 2011. It was initiated by M3.9 earthquake followed by two magnitude larger than 5.0 quakes and the activity lasted for a couple of weeks. No active earthquake faults have been recognized, and no significant seismic activities or magnitude larger than 5 events have been observed previously except the ones observed in 1960s due to filling of the reservoir. The question is if the seismicity observed in October 2011 was related to the dam reservoir. To address question, we will examine the stress state of the area before and after the seismicity. As a first step of the study, we relocated 222 earthquakes observed in this area from Mach to November 2011. Then we analyzed 24 focal mechanisms to etch the shape of fault line. The results showed the epicenters moved 1.5 km eastward and two major faults, one with strike between 160 and 175 degrees, and another with strike between 180 and 195 degrees, were illuminated. Next we calculate the Coulomb failure function(ΔCFF) if the seismicity can be explained by static stress change due to the seismic activity occurred in March. The results indicate that although M5.4 and M5.2 events were possibly triggered by M3.9 and M5.4 events respectively, and the successive aftershocks were triggered by both M5.4 and M5.2 events, It might be difficult to trigger M3.9 earthquake just because of the static stress change due to the seismicity in March 2011. To figure out other causes which can trigger M3.9 event, we examined a dynamic stress triggering and found there was about 8kPa dynamic stress change due to a remote earthquake. As the next step, we will examine if there is any significant pore pressure change so that the seismicity can be triggered by such a small stress change.

Keywords: Seismic activity, Coulomb failure stress change, Dynamic stress change, Pore water pressure, Shear wave anistropy, Hida mountains

Japan Geoscience Union Meeting 2015
(May 24th - 28th at Makuhari, Chiba, Japan)

SSS30-P13 Room:Convention Hall Time:May 25 18:15-19:30

Development of the quasi-dynamic cycle simulation code including both great and small earthquakes

TAKASAKI, Keisuke[1*] ; HIRAHARA, Kazuro[1] ; OHTANI, Makiko[1]

[1]Graduate School of Science,Kyoto University

The magnitude-frequency relation of earthquakes is formulated as Gutenberg-Richter law (GR law). The b values in the GR law take different ones depending on the regions and also show temporal changes. If the b value increases,the number of large earthquakes relatively decreases,and vise versa.

Nanjo et al.(2012) reported that the b value had decreased during a period of ten years before great earthquakes,such as 2011 Tohoku and 2004 Sumatra earthquakes. They suggested that the decrease of the b value can be phenomenon before the occurrences of great earthquakes.

Tormann et al.(2015) reported that the b value,which increase after the 2011 Tohoku earthquake,decreased to the value nearly equal to that before the earthquake.

Although the physical mechanism of the temporal change in the b value has remained unclear,small but many earthquakes may give some effect on the occurrence of great earthquakes or at least the change in the b value can be an indicator of stress state in the focal regions of great earthquakes. It may lead to forcasting great earthquakes that we understand the physical mechanism of the temporal change in the b value. One of ways for clarifying the physical mechanism is to simulate earthquake cycles,which include not only great earthquakes but also small ones,and reproduce the spatio-temporal change in b value for a variety of rate- and state friction models.

Since interseismic period is much longer than coseismic one,the adaptive time-step control Runge-Kutta method is usually used in the present simulations. While the time-steps take small values around the coseismic period with large slip rates,the time-steps take larger ones in the interseismic period with smaller slip rates. Most of present simulations reproduce only great earthquakes,not including many earthquakes with different magnitudes.

If the small earthquakes whose magnitude-frequency relation obeys the GR laws are simulated in addition to great ones,the earthquakes always occur and requires small time-steps in the whole period,leading to the huge computational costs. Thus,we have to reduce the costs for small earthquake simulations in particular to realize the realistic cycle simulations of earthquakes with a variety of sizes.

As noted above,it is the key issue to reduce the computational costs in order to simulate the spatio-temporal change in the b value in the focal region during great earthquake cycles. In our simulations,we use the boundary element method and the quasi-dynamic approximation(Rice,1993).

In addition to the problem of time-steps,the time consuming part is the product calculation of the slip response function matrix and the slip velocity vector. When plate interface is divided into the N small subfaults, the computational cost is O($N*N$). N become much larger when including small earthquakes. We apply H-matrices method to the product part in cycle simulations,which reduces the memory size and the CPU time to O(N)-O($N\log N$)(Ohtani et al.,2011).

As described above,we have to use small time-steps in cycle simulations including also cycles of many small earthquakes,and the computational costs become huge. For this reason,RSQSim(Dieterich and Richards-Dinger,2010) code has been developed. In this study,however,we try to develop another code which performs the same quasi-dynamic cycle simulations for large earthquakes as in the usual ones and the simplified ones for small earthquakes. Namely,when the stress at a patch of small earthquake reaches a certain value,the stress is released and the slip and slip velocity are given in proportion to the stress drop.

In the talk,we give some details of the computation and evaluate our model. Furthermore,we add discussion on the current problems and th future perspectives of our approach.

Keywords: earthquake cycle, numerical simulation, Gutenberg-Richter law, fast computation

Japan Geoscience Union Meeting 2015
(May 24th - 28th at Makuhari, Chiba, Japan)

SSS30-P14 Room:Convention Hall Time:May 25 18:15-19:30

Recurrence intervals of Miyagi-oki earthquakes after the 2011 Tohoku-oki earthquake based on numerical simulations (II)

NAKATA, Ryoko[1*] ; ARIYOSHI, Keisuke[1] ; HYODO, Mamoru[1] ; HORI, Takane[1]

[1]JAMSTEC

Along the Japan Trench, interplate earthquakes (M7.1-7.4), which described as Miyagi-Oki earthquakes have occurred with recurrence intervals of approximately 30-40 years. Although it had passed only 5.5 years since the latest Miyagi-Oki earthquake on August 2005, the source regions of the past Miyagi-Oki earthquakes again ruptured during the 2011 M9.0 Tohoku-Oki earthquake. Coseismic rupture propagated to Fukushima-Oki, where three M7.3-7.5 earthquakes occurred on 1938. And 30 minutes after the mainshock, the largest aftershock (M7.6) occurred in Ibaraki-Oki, where M<7 earthquakes repeatedly occurred in the past.

Previous two studies based on numerical simulations using the composite law, which is a type of rate- and state-dependent friction law showed contrasting estimations for occurrence of the next (just after the Tohoku earthquake) Miyagi-Oki earthquake. But, both simulations estimated coseismic slip during the mainshock at the correspondent Miyagi-Oki region was much larger than that of seismic and geodetic observations. Then, we numerically simulated cycles for occurrences of seismic and aseismic events along the Japan Trench with the 3D geometry of the Pacific plate using the aging law, which is another type of the friction law. We assumed a slightly stronger frictional heterogeneity at shallower part of the Miyagi-Oki region over a wide range instead to assuming a very strong heterogeneity near the trench as the two previous studies. And we used a small value of seismic radiation damping factor to reproduce shorter propagation time during the M9.0 mainshock.

As a results, we reproduced reasonable coseismic slip at the Miyagi-Oki region, and significantly large coseismic slip along the trench. Models which qualitatively reproduced several observation characteristics showed that time interval between the M˜9 earthquake and the first Miyagi-Oki earthquake after the M˜9 earthquake tend to be shorter than the average recurrence interval observed before the M˜9 earthquake. It corresponds to a previous study of Kato and Yoshida [2011]. Recurrence of M7 class earthquakes after the M9 earthquake should continuously be studied by various models. Observations around M7 class earthquake areas are also important.

Japan Geoscience Union Meeting 2015
(May 24th - 28th at Makuhari, Chiba, Japan)

SSS30-P15 Room:Convention Hall Time:May 25 18:15-19:30

Improvement of an experimental equipment for vibrating a sand-pile -For understanding the mechanism of landslides-

NAKAYAMA, Masayuki[1*] ; KAWAKATA, Hironori[1]

[1]Ritsumeikan Univ.

Landslides have been often triggered by seismic shake and/or rainfall. For example, the 2008 Iwate-Miyagi Nairiku Earthquake induced a massive landslide near Aratozawa Dam in Miyagi prefecture. However, the mechanism of earthquake-induced landslides has not been revealed yet due to the complexity of various factors: geography, geology and groundwater.

Yoshioka (2003) studied the relation between the frequency and the size of avalanches in sand-pile experiments. Nakayama et al. (2014, SSJ) investigated a behavior of a sand-pile when vibration was applied in order to understand the mechanism of the earthquake-induced landslides. They prepared a PET bottle which was cut along its bottom with a cap including a small hole and fixed them on a stand. They dropped dry sand particles in a PET bottle through the small hole and made a sand-pile on an acrylic case on whose bottom a buzzer was attached. Using the buzzer, vibration was input to a sand-pile and recorded the visual behavior of the sand-pile. The size of the sand pile was 60 mm in diameter and 20 mm in height. Two kinds of avalanches were found in their experiments, that is to say, avalanches of the grains of sand independently falling along the sand-pile surface and avalanches of thin sand layers sliding downward along the sand-pile surface. However, such avalanches were not observed on some cases.

In this study, we carried out some more experiments, and went through their experimental condition. We found the spatial variation of amplitudes and dominant frequency of the vibration. In addition, we cannot see the detailed process of avalanches because of lower spatio-temporal resolution.

Then, we try to improve the experimental equipment. For example, we replaced a buzzer to a new one which can change the amplitude and dominant frequency. We changed a shape of the base where we made a sand-pile to reduce spatial variation of the vibration. In addition, we installed a high-speed camera to investigate the process of avalanche in detail.

Acknowledgments:
We are grateful to Dr. I. Doi and Dr. N. Takahashi for their advice and support.

Keywords: lanslide